Crustal Deformation and the Seismic Cycle across the Kodiak Islands, Alaska

Jeanne Sauber, Planetary Geodynamics Laboratory, NASA's Goddard Space Flight Center, Greenbelt, MD, 20771

Gary Carver, Department of Geology, Humboldt State University, Arcata, CA, 95521

Steven Cohen, Planetary Geodynamics Laboratory, NASA's Goddard Space Flight Center, Greenbelt, MD, 20771

Robert King, Department of Earth, Atmospheric, and Planetary Science, Massachusetts Institute Of Technology, Cambridge, MA, 02139

Abstract

The Kodiak Islands are located approximately 120 to 250 km from the Alaska-Aleutian Trench and are within the southern extent of the 1964 Prince William Sound (M_w = 9.2) earthquake rupture zone. Here we report new campaign GPS results (1993-2001) from northern Kodiak Island. The rate and orientation of the horizontal velocities, relative to a fixed North America, range from 25.3 ± 1.4 mm/yr at N32.9°W ± 2.5° to 8.5 ± 1.0 mm/yr at N59.7°W ± 6.5°. In addition to the northern Kodiak data, we analyzed data from three southern Kodiak Island stations. The inland stations from both the northern and southern networks indicate a counterclockwise rotation of the velocity vectors. These results are consistent with the hypothesis that the difference between the Pacific-North American plate motion and the orientation of the down going slab would lead to 4-8 mm/yr of left-lateral slip above the unlocked, down-dip portion of the main thrust zone. The northern and southern Kodiak geodetic data are consistent with a model that includes the viscoelastic response to (1) a downgoing Pacific plate interface that is locked at shallow depths, (2) local coseismic slip in the 1964 earthquake, and (3) interseismic creep down dip from the seismogenic zone. Based on the pre-1964 and post-1964 earthquake history, as well as the pattern of interseismic earthquakes across the plate boundary zone, we hypothesize that in southern Kodiak some strain is released in moderate to large earthquakes between the occurrences of great earthquakes like the 1964 event.

Geologic and Tectonic Setting

The motion of the Pacific plate relative to the North American plate is at a rate of about 57 mm/yr at N22°W [*DeMets et al.*, 1994]. The Kodiak Islands span a region approximately 120 to 250 km from the Alaska-Aleutian Trench (taken here to be the eastern extent of the 4000 m or 5200 m bathymetric contour). The subducting Pacific plate is thought to have a shallow dip (<10°) from the Aleutian trench northwestward to 30-40 km below Kodiak Island based on seismicity [*Davies et al.*, 1981; *Pulpan and Frohlich*, 1985] and the geological structure suggested from a deep crustal transect [*vonHuene et al.*, 1999] (Figure 1). From the northern to the southern part of the island the distance from the Aleutian trench to the eastern coast of Kodiak Island narrows by about 10% (Figure 1). This change probably reflects a slight steepening of the dip of the down going Pacific plate under the southern part of the island. The average trend of the trench off northern Kodiak is approximately N60°E which gives a trench perpendicular motion more westerly than the relative plate motion vector by about 8°. The difference in orientation between the trench normal and the relative plate motion has potential implications for the crustal deformation patterns [*McCaffrey et al.*, 2000].

All of the Kodiak Islands lie within the southern extent of the 1964 Prince William Sound (M_w = 9.2) earthquake rupture and aftershock zone. Prior to the 1964 earthquake, in 1900, a M_S = 7.7 earthquake occurred in the southeastern part of Kodiak [*Gilpin et al.*, 1994; *Gilpin*, 1995; *Doser et al.*, personal communication, 2004]. *Nishenko and Jacob* [1990] suggest a recurrence interval of approximately 60 years between periods of increased activity that last as long as 10 years based on large and great earthquakes felt on Kodiak Island during the last 200 years; they considered all of the Kodiak Islands as one segment of the Alaska-Aleutian subduction zone. Recently, several large earthquakes (M_w = 7.0, in 1999; M_w = 6.5 in 2000; M_w = 7.0 in 2001) have occurred in the southern part of the

Kodiak Islands as well [*Ratchkovski and Hansen,* 2001; *Hansen and Ratchkovski,* 2001]. The Harvard and U.S. Geological Survey (USGS) Centroid Moment Tensor solutions (CMTs, *Dziewonski and Woodhouse,* 1983; *Ekstrom,* 1994; http://neic.usgs.gov/neis/sopar) for the events are given in Figure 2. The focal mechanisms between Nov. 1977 and Feb. 2004 indicate a combination of reverse faulting events on northeast-southwest striking planes and left-lateral strike-slip events at roughly trench-parallel orientations (Figure 2). These earthquakes, as well as earthquake focal mechanisms from 1964 – 1979, are discussed in relation to the 1964 earthquake in *Doser et al.,* [2002]. They found that the earthquakes between 1964 and 1979 were characterized by more normal and normal-oblique mechanisms. The earthquakes since 1964, as well as historical earthquakes reported in *Gilpin* [1995], indicate that the southern Kodiak Island region has had moderate to large earthquakes more frequently than northern Kodiak both prior to, and following, the 1964 earthquake.

The Kodiak Islands are part of a large subduction complex that comprises the eastern Aleutian forearc; the islands form the subaerial part of a broad topographic ridge that includes a Mesozoic-Cenozoic accretionary complex (Figure 1). The Kodiak Seamount (24 Ma) shown in Figure 1 is part of the Kodiak – Bowie seamounts, a hot spot chain that transects the Gulf of Alaska; it is the oldest seamount still exposed prior to subduction. *vonHuene et al.* [1999] hypothesized that a thickened and thermally hot oceanic crust in this region is a more buoyant segment than adjacent crust and may have acted as a second seismic asperity in the 1964 earthquake (the primary asperity and epicenter was in the Prince William Sound area).

In the next section, we report horizontal velocities and uplift rates estimated from GPS measurements made between 1993 and 2001 across the northern region of Kodiak. To put these results in a regional context we included in our analysis GPS measurements made by *Savage et al.,* [1999] across the southern portion of the Kodiak Islands and measurements from the two permanent stations

(KOD1 and KODK). We used these geodetic results to further address the following questions: (1) how do the ongoing crustal deformation rates vary as a function of distance from the trench? (2) Are there differences in the deformation rates between northern and southern Kodiak? (3) What was the magnitude of 1964 coseismic slip near northern and southern Kodiak? (4) What is the seismic history of moderate to large earthquakes in northern and southern Kodiak? Are there differences between these two regions? (5) Does the rate of horizontal and vertical deformation vary as a function of time since the 1964 earthquake?

Global Positioning System Measurements and Analysis

To estimate station velocities we have used observations from eight locations on Kodiak Island acquired with varying occupation scenarios between 1993 and 2001 (Table 1), along with observations from the two Kodiak permanent GPS stations. We surveyed five primary stations in the northern part of the island (PASA, MILB, CLAM, KODI, and SKI0) three or four times between 1993 and 2001, occupying most of these for 6-8 hours on 1-4 days but KODI continuously for the length of each survey. In 1995, 1997, and 1999 these observations were made as part of an education outreach program with Kodiak Island High School [*Stockman et al.*, 1997; *Sauber et al.*, 1998; E. Linscheid http://137.229.234.24/nasa/index.html]. There are two extended "geodetic footprints" in our northern Kodiak geodetic network (Table 1). The KODI footprint includes a station, KODV (10 m from KODI), that was previously measured with very-long-baseline-interferometry (VLBI) between 1984 and 1990 [*Ma et al.*, 1990]. The footprint also includes the permanent station KODK (located within 1 km of KODI) constructed in late 1998 as part of an educational and outreach program with NASA's Goddard Space Flight Center, Kodiak Island High School, and Thales Navigation. The second extended footprint includes our station MILB located near the U.S. Coast Guard station KOD1, installed in 1997 as a Continuously Operating Reference Station (CORS) of the National Geodetic Survey. Additional

nearby stations within the two footprints were surveyed once or twice for back-up in case the primary site was destroyed (Table 1).

The U.S. Geological Survey (USGS) surveyed three stations (KRLK, AHKI, SITK) in the southern part of Kodiak Island as well as additional stations on the Alaska Peninsula in 1993, 1995, and 1997, occupying each station for at least 48 hours [*Savage et al.,* 1999]. The southern Kodiak stations were surveyed again in 2001 by the USGS and the University of Alaska. However, since there were large nearby earthquakes between 1999 and 2001, we used only the Kodiak Island observations through 1997 in our analysis.

We obtained the velocities of the GPS stations using the GAMIT/GLOBK software [*King and Bock*, 2003; *Herring,* 2003] and the procedure described by *McClusky et al.,* [2000], combining the observations from our field receivers with those of the global IGS network processed at the Scripps Orbit and Permanent Array Center (SOPAC) [*Bock et al.,* 1997]. To define a North America reference frame, we minimized the horizontal velocities of 11 stations within the non-deforming regions of the North America and Pacific plates (Table 2). The residual motion of these 11 stations is 0.8 mm/yr.

In order to evaluate the uncertainties of our velocity estimates, we computed and examined time series of position within each survey and over the full span of our data for stations with at least 3 observation time periods (Figure 3). With the *a priori* uncertainties we assigned to the phase observations, the normalized rms of the long-term repeatability has a median value of about 0.7, which we have found from analysis of similar but more extensive data sets to result in realistic uncertainties in velocities estimated from two or more years of observations (see, e.g., *McClusky et al.,* 2000). For those stations in the Kodiak network whose unscaled nrms scatters were greater than 1.0 we down-weighted the position estimates to achieve values closer to 0.7. Our estimates of vertical motions are less reliable than those for horizontal motion in part because of larger uncertainties in the estimates of height from

the short observation scenarios used for many of the surveys and in part because of larger vertical uncertainties in reference frame.

Velocity results

The estimated velocities in a North America fixed reference frame are given in Table 3 and the well-determined horizontal velocities are shown in Figure 2. The station velocities are plotted as trench-normal and trench-parallel components in Figure 4 and listed in Table 3. For both the northern and southern Kodiak stations, the trench-normal velocities decrease nearly uniformly with distance from the trench (Figure 4).

We have a small number of stations located within 1 km of the extended footprints to assess the internal consistency of the velocities. The stations within the individual KOD1 and KODI footprints have similar horizontal velocities within the 1σ level of uncertainty (Table 1); the vertical uplift rates, however, show greater variability. From a solution in which the estimated vertical rates of the nearest North American stations (at Penticton, B.C., and Fairbanks) are less than 3 mm/yr, we estimated uplift rates of 12-18 mm/yr for stations between 170 and 230 km from the trench. There is 10 mm/yr of differential uplift between CLAM/KODI/KODK/SKI0/KRLK and KOD1/MILB/SITK. The individual station vertical results are included for completeness. Due to the large variability in these results, as a function of distance from the trench, we are more confident of the horizontal velocities.

Plate normal motion or trench parallel component of slip

The map view of the horizontal velocities given in Figure 2 illustrates the counterclockwise rotation of the velocity vectors for stations in the west relative to the eastern coastal stations. If we hypothesize that the orientation of the down going slab is primarily controlled by the orientation of relative motion between the Pacific and North American plates, we would expect the velocities above the locked portion of the plate interface to be at approximately the N22°W orientation. To test this, we

rotated the velocities of Table 1 into a plate motion parallel component and a plate perpendicular component (Table 3). Most of the Kodiak stations indicate a plate parallel component of 4-6 mm/yr.

An alternate factor that may control the orientation of the down going slab is the geometry of the Aleutian trench. The orientation of down going Pacific plate motion would lead to compressional strain at N30°W; further inland the trench-parallel strain would be relieved as left-lateral slip on upper plate faults. We resolved the data into trench perpendicular (N30°W) and trench parallel components (N60°W) (Table 2 and Figure 4). The Kodiak Gulf of Alaska coastal stations (SITK, PASA, KOD1) have orientations that are close to the trench-normal (N30°W) but MILB indicates a velocity at an orientation (N20.8°W ± 5.5°) that is closer to that predicted for the relative plate motion (~N22°W). The trench parallel component increases with distance from the eastern coast. These results suggest distributed shear strain accumulation that could be relieved on individual faults or distributed over a broad region. The Kodiak Island and Narrow Cape faults are the largest mapped trench parallel faults in this region. Mapping and paleoseismic studies of the Narrow Cape fault show it has produced predominately left-lateral strike-slip displacement during the Holocene [*Carver et al.*, 2003].

Modeling of Kodiak Island Geodetic Observations

Although the epicenter for the 1964 earthquake was in the Prince Williams Sound area (between Anchorage and Valdez) of south central Alaska, the aftershock area extended ~300 km to the east and ~800 km to the southwest (to south of the Kodiak Islands). Two areas of high slip in the 1964 event correspond to seismologically determined areas of high moment release: (1) the Prince William Sound asperity had an average slip of 18 m and the Kodiak asperity had an average slip of 10 m [*Johnson et al.*, 1996; *Christensen et al.*, 1994; *Holdahl and Sauber*, 1994]. In our discussion of the factors that contribute to ongoing crustal deformation across Kodiak we consider only the contribution of the

southern "Kodiak asperity". *Wells et al.*, [2003] noted that areas of high coseismic slip commonly occurred beneath the prominent gravity lows outlining a deep-sea terrace low. The location of the Kodiak asperity does not seem to be associated with a prominent forearc basin gravity low.

In addition to the trench parallel variability in the coseismic slip in the 1964 earthquake noted above, changes in the coseismic slip and interseismic locking depth as a function of distance from the Aleutian Trench occur as well. In general, the seismogenic zone along the subduction plate interface is bounded by the upper and lower stability transition depths [e.g. *Scholz,* 1990]. The seaward updip limit is important for tsunami generation and the downdip limit is important for seismic hazard because it is used to infer the landward limit of the seismic source zone (e.g. *Oleskevich et al.,* 1999). Since the boundary between the region of coseismic uplift and subsidence in the 1964 earthquake occurred on the eastern portion of the island, earlier studies suggested that Kodiak Island is above the transition zone between interface slip in large earthquakes, post-seismic creep, and aseismic creep at depth [*Ma et al.,* 1990; *Gilpin et al.,* 1994; *Gilpin,* 1995; *Stockman et al.,* 1997; *Savage et al.,* 1999; *Zweck et al.,* 2002]. These earlier Kodiak geodetic observations and modeling, however, hypothesize different downdip limits for coseismic slip and interseismic locking somewhere beneath Kodiak Island.

We used aftershocks and tsunami studies of the 1964 earthquake, as well as thermomechanical models to give us an approximation of the updip limit of significant coseismic slip. Aftershocks following the 1964 earthquake suggest that significant coseismic slip started at approximately 100 km from the trench (toward northern Kodiak) [*Algermessen et al.,* 1969]. *Oleskevich et al.,* [1999] estimated the 100-150^{0}C temperature isotherm limit for clay dehydration between the Kenai Peninsula and Kodiak to be 80-160 km landward from the trench. In the northern Kodiak region there are some large earthquakes near the 1600 m contour but large earthquakes have not occurred near the trench over

the last 20+ years (Figure 2). In contrast, in southern Kodiak, moderate to large earthquakes have occurred between the trench and the Alaska Peninsula (Figure 2).

The depth of the Aleutian trench ranges from about 4000 m near the northeastern part of the Kodiak Islands to 5200 m a little farther south [*Beikman,* 1980]. The depth and curvature of the dipping slab in our finite element model matches the dip of the upper slab surface inferred from background seismicity in the region of Kodiak Island. However, the dip in our finite element model, near the trench, may be too steep. The dip of the shallow portion of the slab used in the finite element model is about as shallow as possible given the necessity to avoid an extreme aspect ratio of the elements that would create a numerical instability.

In addition to the megathrust fault (down-going Pacific plate), Holocene surface faulting in and near the northeastern portion of the Kodiak Islands has been mapped offshore on the Kodiak Shelf fault system [*Plafker et al.,* 1994] as well as within the Narrow Cape region [*Carver et al.,* 2000, 2003] near the station PASA (Figure 1 and 2). The Border Ranges fault traverses on-shore along the northwest coastline of the Kodiak Islands (Figures 1 and 2) but no clear evidence of Holocene slip on this fault system has been observed [*Gilpin,* 1995]. We assumed motion along the plate interface is the primary source of interseismic strain but we considered slip on the upper plate faults in our interpretation of horizontal velocities.

Over the time and spatial scale of the surface deformation measurements in this study, the response of the Earth to tectonic loading depends on the rheological structure of the crust and upper mantle. The time-dependent response of the Earth has been shown to be important in Alaska for modeling geodetic data [*Brown et al.,* 1977; *Wahr and Weiss,* 1980; *Sauber et al.,* 1993; *Savage and Plafker,* 1991; *Cohen,* 1996; *Taylor et al.,* 1996; *Zheng et al.,* 1996; *Freymueller et al.,* 2000; *Sauber et al.,* 2000, *Zweck et al.,* 2000; *Freymueller et al.,* 2001]. Two time-dependent processes are particularly

important in this region of large and great earthquakes. These are fault creep occurring down-dip of the coseismic rupture plane and viscoelastic shear flow in the ductile portions of the lower crust and upper mantle [see summary in *Cohen,* 1999]. Both of these mechanisms are stimulated by the coseismic transfer of stress from the shallow seismogenic portions of the Earth to greater depths. To evaluate alternate interseismic and post-seismic mechanisms that could account for our geodetic observations between 1993 and 2001, we calculated the predicted average surface displacement rate for alternate Earth models. We used primarily a two-dimensional plain strain finite element grid in TECTON [*Melosh and Raefsky,* 1981] for these calculations. The finite element grid across the plate boundary includes a shallow dipping subducting slab and both an oceanic crust-mantle and a continental crust-mantle (Figure 5a). Because of our uncertain knowledge of the Earth's response to tectonic loading on the time scale of years, we explored alternate interface slip distributions and rheological models for the post-1964 coseismic and interseismic time periods. Due to the low viscosities in the lower crust and upper mantle (~$10^{19\text{-}20}$ Pa s) inferred from most studies in Alaska, we assumed the current response to major late Pleistocene deglaciation and sea level rise on Kodiak Island to be insignificant. Recent glacial fluctuations on Kodiak Island are small and are not modeled as well.

Simplifying the formulation given by *Cohen* [1999], we calculated the surface velocity over our time frame of interest due to the viscoelastic response to three major conceptual elements: (1) plate motion over the last 30+ years, (2) the 1964 earthquake and (3) down-dip creep below the region of maximum slip in the 1964 earthquake. The strain accumulation associated with the first term (1) was calculated as the viscoelastic response to back-slip on the shallow portion of the plate interface. The second term is the viscoelastic response to coseismic slip in the 1964 earthquake. Although the coseismic term is dependent on the (coseismic) slip distribution assumed as well as the viscosity structure, in general this term is smaller than (1), especially 30+ years after the earthquake. The third

term, creep on the plate interface, can be time-dependent as well. Studies from the Prince William Sound area have suggested this is an important mechanism [*Brown et al.,* 1977; *Cohen,* 1996; Cohen *Cohen et al.,* 1995; *Freymueller et al.,* 2000; *Cohen and Freymueller,* 2001]. Although we explore a range of creep models, greater spatial and temporal resolution of surface velocities is needed to resolve the time-dependent changes in down-dip creep.

Coseismic slip in the 1964 earthquake

Since the occurrence of the 1964 earthquake, numerous models of slip in the 1964 earthquake have been proposed and we will not attempt to summarize all the studies here. As mentioned earlier, the more recent models include a region of high slip referred to as the "Kodiak asperity" but studies differ in the location and magnitude of slip in this asperity [*Christensen and Beck,* 1994; *Holdahl and Sauber,* 1994; *Gilpin et al.,* 1994; *Gilpin,* 1995; *Johnson et al.,* 1996]. *Gilpin* [1995] included the most extensive Kodiak tide gauge and geologic data set and he inverted for slip across three different regions of Kodiak Island but not other regions (i.e. the Prince William Sound region that slipped in the 1964 earthquake). Gilpin's results also suggest that slip offshore extending to below northern Kodiak Island was larger than in southern Kodiak.

The geologic and geodetic measurements used as constraints in the recent coseismic models actually bracket up to 14 months of slip. Thus estimates for "coseismic slip" include short-term post-seismic processes such as fault slip in aftershocks, both on the plate interface and within the surrounding region, down-dip creep, and any very short-term anelastic response of the Earth. Also, it is important to note that for most of the coseismic slip models the vertical displacements (from offset of barnacles, tide gauge data, leveling) were the primary constraint. For more recent data used to estimate interseismic strain rates, such as our geodetic observations, the horizontal rate of deformation is the better constrained component.

In this section we refine the coseismic slip models suggested by earlier studies to make our two-dimensional (2-D) models specific to the two regions with geodetic observations. We used the tide gauge data summarized in *Gilpin* [1995] for the "northern" and "southern" Kodiak. The 1964 coseismic subsidence and uplift values for the north (black, in Figure 6) and south (red) are clearly different. For Model 1 (MD1) we used a coseismic slip of 10 m for the depth range between 11 and 22 km (modified from *Holdahl and Sauber*, 1994; *Johnson et al.,* 1996). We assumed a linear transition to zero slip between 9 and 11 km and between 22 and 30 km (Figures 5a and 5b, solid line without creep between 30 and 90 km). In such a model, slip in the 1964 earthquake was shallow and any post-seismic response was associated with a fairly shallow (< 40 km) low viscosity zone. The second model MD2 is partially based on the maximum slip in northern Kodiak given in *Gilpin* [1995] (Figures 5a and 5b); the coseismic slip is higher (MD1 above multiplied by 1.4 m) and we assumed short-term post-seismic creep below the seismogenic zone (up to 3 m between depths of 22 and 90 kms). In this model we assumed a deeper (> 90 km) low viscosity zone. For southern Kodiak we multiplied both MD1 and MD2 models by 0.5 (half the coseismic slip as suggested by earlier studies). The predicted coseismic displacements due to these alternate coseismic slip distributions are compared in Figure 6. Although the two coseismic models would place different boundary conditions on the top of the asthenosphere right after an earthquake, the available vertical displacements at the surface can not distinguish them.

Interseismic model (1993-2001)

As discussed above, a number of mechanisms could influence the surface deformation rates obtained in this study, ~30-40 years following the 1964 earthquake. There are numerous studies of the post-seismic response to the 1964 earthquake especially in the Kenai region (*Cohen et al.,* 1995 and see summary in *Freymueller et al.,* 2000). Additionally, in the Kodiak region, *Gilpin et al.,* [1994] and *Gilpin* [1995] used permanent and temporary tide gauge data from the islands to estimate a down-dip,

post-seismic creep of approximately 3 meters during the 25 years following the earthquake. This is about the amount of creep inferred for the Kenai region over a similar time period [*Cohen et al.,* 1995; *Freymueller et al.,* 2000]. Based on their analysis of tide gauge data, *Savage and Plafker* [1991] postulated that in addition to down-dip creep, a slower viscoelastic relaxation of the low viscosity mantle could be important over a longer time scale. We included the viscoelastic response to 1964 slip in both end member models, albeit at different depths.

Elastic dislocation model

Locking of the plate interface at shallow depths is assumed to exert the greatest influence on the interseismic rate of deformation over 30 years after the 1964 earthquake. For a point of reference we present the elastic dislocation model used by *Savage et al.,* [1999] to represent back-slip at the relative plate rate on a shallow main thrust zone [*Freund and Barnett,* 1976; *Savage,* 1983]. The elastic slip model is shown Figure 5c and the comparison to data is shown in Figure 7a,b. *Savage et al.*[1999] used a nonlinear inversion program to determine the parameters for a dislocation model which best fits their southern Kodiak data. They assumed a dip of 5° along the locked plate interface. The locked zone width of approximately 152 km (57 km to 209 km downdip, Figure 3 *Savage et al.,* 1999) and a back-slip rate of about 57 mm/yr were estimated. Their locked zone was between depths of 5 and 18 km (Figure 5c). If the elastic profile is shifted relative to the trench (the assumed zero depth is further east due to, for instance, a shallower dip) the elastic model will fit the data better near the locked main thrust zone. The elastic model however does not account for data further inland. The predicted trench normal rate of deformation from northern and southern Kodiak shown in Figure 7a illustrates the important contribution the shallow locked zone makes to ongoing strain accumulation but the data/model discrepancy also suggests that other processes could contribute.

Predicted time-dependent surface displacement rate

For the two MD1 models, we consider two processes, the elastic response to ongoing plate motion and the viscoelastic response to coseismic slip in the 1964 earthquake (see summary in Table 4). In this model the lower crust and/or upper mantle is assumed to respond viscoelastically and most of the elastic layer ruptured during the 1964 earthquake. In MD1a we used the coseismic region as a proxy for the region that is locked during the interseismic time period. Specifically, between 11 and 22 km we imposed 57 mm/yr of back-slip and between 9 and 11 km and 22 and 30 km, the imposed plate rate of back-slip was reduced to zero. For model MD1b, we used a shorter locked zone that is closer in extent to the elastic model of Savage. In the MD1 models, the transient component of surface deformation is primarily due to the time-dependent viscous relaxation of a shallow (> 38 km) low viscosity zone instead of time-dependent, down-dip creep. For our reference model given in the figures we assumed a viscosity of η of 5×10^{19} Pa s and rigidity (G) of 0.6×10^{19} Pa. This corresponds to a Maxwell time, τ, of ~ 26 years, where $\tau = \eta/G$. The influence of the assumed viscosity η is discussed later. Post-seismic relaxation of the 1964 displacement would cause subsidence and horizontal motion away from the trench above the 1964 rupture. The predicted horizontal and vertical displacement rates for MD1a,b are compared to the horizontal and vertical data and the elastic model in Figures 7a and 7b. The MD1a,b and the elastic model predictions are similar to the observed horizontal data near the locked main thrust zone but trench directed motion on the Alaska Peninsula is not predicted (1993-2001, http://quake.wr.usgs.gov/research/deformation/gps/auto/KatmaiKodiak). Future measurements on the Alaska Peninsula and along the western coast of Kodiak would provide more robust constraints.

In the MD2 suite of models the low viscosity layer is deeper (≥ 90 km) and post-seismic creep from the base of the seismogenic zone down to 90 kms is included and evaluated (Figure 5a, d and Table 4). In MD2a, b (Table 4) we assumed that the region of high coseismic slips was also the region that

was locked during the interseismic time period (i.e. the MD2 coseismic model). For the MD2c, d we assumed the region of full interseismic coupling was slightly smaller than the region of high coseismic slip in the 1964 earthquake; this is, closer to the locked region of *Savage et al.,* [1999] but the MD2c, d viscoelastic model includes down-dip creep as well. We calculated the response to 10-60 mm/yr of creep between the down-dip extent of the locked zone to 90 km. A model with little (MD2a) or no creep between 30 and 90 km predicts a higher horizontal rate of deformation (arc directed) than observed in northern Kodiak (Figure 8a). At the other extreme, a model (not shown) that includes 60 mm/yr of creep under predicts the horizontal rate of deformation directed arc-ward. Since the amount of coseismic slip is different between the north and south we included the region-specific postseismic relaxation due to coseismic slip for the calculations; thus the post-seismic viscous relaxation is hypothesized to be smaller in southern Kodiak. Additionally we hypothesize that the magnitude of creep scales as a function of coseismic slip as well. MD2c in red represents the predicted horizontal rates for southern Kodiak (Figure 8a). For the model that best predicts the northern horizontal data (MD2c) we plotted the individual contribution from each of the deformation mechanisms (Figure 8c). The vertical data are best predicted by the MD2 a,b models with the wider locked main thrust zone.

Each of these models predicts different horizontal velocities for the Alaska Peninsula region (Figure 8a) as well. The stations from the Alaska Peninsula in the Katmai volcano region have small, horizontal velocities (3-4 mm/yr) that are primarily trench directed in a North America fixed reference frame (1993-2001, http://quake.wr.usgs.gov/research/deformation/gps/auto/KatmaiKodiak). These results are similar to that observed in the Kenai which have been attributed to dip-slip creep on a portion of the plate interface below the locked main thrust zone [*Freymueller et al.,* 2000]. The higher creep models (MD2b,d) however, over predict the amount of trench directed motion on the Alaska Peninsula.

Variable viscosity values and the preferred model

The post-seismic component is small relative to interseismic strain and creep but we explored various viscosity values to test the uniqueness of the viscosity used to calculate the postseismic response to the 1964 earthquake. We varied the lower crust/upper mantle viscosity between 10^{19} and 5 x 10^{20} Pa s. With a viscosity of 10^{19} Pa s the Maxwell time, τ, is just 5 years and for 5 x 10^{20} Pa s, τ = 264 years. The models with the viscosity values of 10^{19} and 5 x 10^{20} Pa s do not approximate the northern Kodiak data. The 10^{20} Pa s model approximates the general drop off in velocity but under predicts the rate as a function of distance from the trench.

Discussion

Sources of time-dependent deformation

Based on our modeling of the geodetic observations, time-dependent creep and possibly post-seismic viscoelastic relaxation may be a significant source of the measured surface velocities. Due to the large uncertainties in our short-term vertical results, we evaluated this conjecture by examining other data from the region of the 1964 earthquake. Long-term and temporary tide gauge measurements have been used as well to estimate uplift rates since the 1964 earthquake [*Savage and Plafker,* 1991; *Gilpin,* 1995; *Cohen and Freymueller,* 2001]. On Kodiak temporary tide gauge measurements have been used to constrain coseismic slip in the 1964 earthquake and additionally these measurements were made between 1965 and 1993, primarily to the west of our northern Kodiak GPS stations [*Gilpin et al.,* 1994; *Gilpin,* 1965]. These vertical measurements show less scatter, as a function of distance of from the trench, than our short-term vertical rates. In Figure 9 we compared the tide gauge uplift values (1965-1993) to the predicted uplift assuming the model parameters given by the elastic and MD1a,b (a) and MD2b,c (b) models. The rate of uplift for the elastic model is much higher than the observed uplift rates for 1965-1993 and the MD1a,b models predict a lower rate of uplift than is observed (Figure 9a). For this earlier time period, the total uplift is better predicted by the model (MD2b) with the higher

creep rate of 25 mm/yr (Figure 9b). Other studies have suggested a time variable uplift rate due to down-dip creep as well. Based on the tide gauge data from Woman's Bay (< 1 km from KODK, KODI and the old VLBI mark), *Cohen and Freymueller* [2001] estimated an average uplift rate of 14 ± 1 mm/yr between 1967 and 1998, but they suggest there is a significant decrease in the uplift rate as a function of time. They estimated an uplift rate of 15 mm/yr for 1985 and 8 mm/yr for 1995.

Recent earthquakes (southern Kodiak 1999-2001, see discussion in introduction) and possibly episodic creep have occurred below the region of high coseismic slip in the 1964 earthquake in the last decade. Around the same time as the earthquakes in southern Kodiak, the "great Alaska earthquake of 1998-2001" occurred in the Anchorage region [*Freymueller et al.*, 2001]. *Freymueller et al.* [2001] hypothesized that the southeast directed surface displacement was due to creep on a segment of the plate interface down-dip from the locked main thrust zone.

Long-term vertical uplift rates compared to our geodetic uplift rates

Landsat-7 and a Shuttle Radar Topography Mission (SRTM) derived digital elevation model (DEM) were used by *Carver et al.* [2003] to identify a coastal marine terrace across the northern portion of Kodiak. The terrace includes broad planar surfaces up to several kms wide that border the modern coast line. The terrace increases in elevation uniformly from about 15 m on the west of the Island (Region III of Figure 1) to about 40 m in the central region (Region II of Figure 1). Based on the assumption that the surface had been cut by shoreline planation during the last interglacial (probably an oxygen isotope stage 5e, 120,000 – 130,000 ka), *Carver et al.* [2003] estimated an average uplift rate of 0.15 mm/yr for Region III to 0.3 mm/yr for Region II (Figure 1). The uplift estimated from the terrace data suggest that within the transition region of the 1964 coseismic uplift and subsidence (Region I of Figure 1) the highest rate of uplift is associated with crustal shortening on upper crustal faults. For instance, at Narrow Cape on Kodiak's northeast coast, the elevation of the terrace is about 80 m and it is

100 m on nearby Ugak Island [*Carver et al.*, 2003]. Mapping and trench studies of several lineaments identified from Landsat-7 and SRTM data show evidence for late Pleistocene and Holocene surface fault rupture in the vicinity of the Kodiak launch facility at Narrow Cape [*Carver et al.*, 2003].

Summary

The new geodetic results reported in this study from northern Kodiak Islands document the change in deformation rates across a transition region between uplift and subsidence in the 1964 earthquake. Earlier VLBI results indicate that a simple elastic dislocation model used to represent interseismic strain accumulation was inadequate to account for the observed horizontal and vertical rates as a function of distance from the trench [*Ma et al.*, 1990]. Later studies further indicate the importance of time-dependent uplift rates following the 1964 earthquake [*Savage and Plafker*, 1991; *Cohen and Freymueller*, 2001]. Permanent GPS stations across Kodiak Island and on the Alaska Peninsula could provide important constraints on down-dip, time-dependent processes. In this study, we suggest that the recent horizontal (trench perpendicular component) and earlier vertical uplift data across Kodiak Island can be accounted for by the viscoelastic response to back-slip representing a locked main thrust zone, down-dip creep, and coseismic slip in the 1964 earthquake. Northern and southern Kodiak have different interface slip histories and interseismic strain predictions. A change in the orientation of the horizontal velocity vectors occurs above the down-dip segment of the locked main thrust zone. We hypothesize that the horizontal, trench-parallel component of slip will be released as left-lateral slip on trench parallel, upper plate faults.

Acknowledgments

Early work on establishing the northern Kodiak geodetic stations and the construction of the KODK station were greatly facilitated by the late Mark Bryant (died on January 14, 2002 at the age of 41) Robert LeMoine and Thomas Clark. The GSFC Alaska team misses Mark's technical expertise, personal integrity and gracious, southern style and we dedicate this paper to his memory.

Eric Linscheid of the Kodiak Island High School has participated in all aspects of this study and most recently has been downloading the KODK station. The U.S. Coast Guard graciously allowed us to locate the KODK monument and receiver at Kodiak Island base. Roy Ecklund put in the geodetic marks for CLAM, SKI and PASA. Robert LeMoine's expert surveying assistance over several summers was greatly appreciated. Nino Fiorentino, Steve Nerem, Steve Fisher, Claudia Carabajal, and Jim Long contributed their field expertise to at least one observation campaign between 1993 and 2001. We thank the numerous students of Kodiak Island High School for their participation in the GPS observation campaigns in 1995, 1997, and 1999, Yehuda Bock and Paul Jamason at SOPAC, Scripps Institute of Oceanography for helping us set-up KODK as an IGS station, and Simon McClusky and Tom Herring for GAMIT/GLOBK assistance. Jim Savage and Karen Wendt kindly helped us acquire the Katmai (1993-1997) GPS data. The numerical calculations reported here were generated using a modified version of the finite element code TECTON developed by H. Jay Melosh. This research was supported by NASA's Solid Earth and Natural Hazards program (921-622-74-10-04), the earlier NASA Dynamics of the Solid Earth DOSE program, and the NASA Goddard Space Flight Center's Director's Discretionary Fund.

References

Algermissen, S. T., W. A. Rinehart, R. W. Sherburne, and W. Dillinger, (1969), Preshocks and Aftershocks of the Prince William Sound Earthquake of March 28, 1964, *Coast and Geodetic Survey Publication* 10-3, vol. II, parts B and C..

Becker, T., and A. Braun, (1998), New program maps geoscience data sets interactively, *Eos Trans. AGU* , 79, 505.

Beikman, H. M., (1980), Geologic map of Alaska: U.S. *Geological Survey Special Map,* scale1:2,500,000 - 2 sheets.

Bock, Y., J. Behr, P. Fang, J. Dean, and R. Leigh, (1997), Scripps Orbit and Permanent Array Center (SOPAC) and Southern California Permanent Array Center (PGGA) in The Global Positioning System for the Geosciences, pp. 55-61, Nat. Acad. Press, Washington, D.C..

Brown, L.D., R. E. Reilinger, S.R. Holdahl, and E.I. Balazs, (1977), Postseismic crustal uplift near Anchorage, Alaska, *J. Geophys. Res., 82,* 3369-3378.

Carver, G.A., R. A. Knecht, R.S. Davis, P. Saltonstall, and J. Sauber, (2000), Holocene sea level changes and resettlement of maritime people in the eastern Aleutian and Kodiak Islands, Alaska, *Eos Trans. AGU 81(48), Fall Meeting Supplement, (abstract),* U61A-04.

~~Carver, G.A., J. Sauber, W. R. Lettis and R. C. Witter, (2003) Use of SRTM and Landsat-7 data~~ to evaluate seismic hazards, Kodiak Island, Alaska, *Eos Trans. EGS-AGU-EUG.*

Christensen, D., and S. Beck, (1994), The 1964 Prince William Sound earthquake: rupture process and plate segmentation, *Pure and Applied Geophysics, 142,* 29-53.

Cohen, S.C., (1996), Time-dependent uplift of the Kenai Peninsula and adjacent regions of south central Alaska since the 1964 Prince William Sound earthquake, *J. Geophys. Res., 101(B4),* 8595-8604.

Cohen, S. C., (1999), Numerical models of crustal deformation in seismic zones, *Advances in Geophysics,* ed. R. Dmowska and B. Saltzman, vol. 41, 133-233.

Cohen, S. C., and J. T. Freymueller, (2001), Crustal uplift in the south central Alaska subduction zone: new analysis and interpretation of tide gauge observations, *J. Geophys. Res.,* 106, 11259-11270.

Cohen, S.C., S. Holdahl, D. Captrette, S. Hilla, and R. Safford and D. Schutz, (1995), Uplift of the Kenai Peninsula, Alaska, since the 1964 Prince William Sound earthquake, *J. Geophys. Res.,* 100, 2031-2038.

Davies, J., L. Sykes, L. House and K.Jacob, (1981), Shumagin seismic gap, Alaska Peninsula: History of great earthquakes, tectonic setting, and evidence for high seismic potential, *J. Geophys. Res.,* 86, 3821-3855.

DeMets, C., R. G. Gordon, D. Argus, and S. Stein, (1994), Effect of recent revisions to the geomagnetic reversal time scale on estimates of current plate motions, *Geophys. Res. Lett.,* 21, 2191-2194.

DeMets, C., and T. H. Dixon, (1999), New kinematic models for Pacific-North American motion from 3 Ma to present, I: Evidence for steady motion and biases in the NUVEL-1A model, *Geophys. Res. Lett.,* 26, 1921-1924.

Dmowska, R., G. Zheng, and J. R. Rice, (1996), Seismicity and deformation at convergent margins due to heterogeneous coupling, *J. Geophys. Res.,* 101(B2), 3015-3029.

Doser, D.I., W.A. Brown, and M. Velasquez, (2002), Seismicity of the Kodiak Island region (1964-2001) and its relation to the 1964 great Alaska earthquake, *Bull. Seism. Soc. Am.*, 92(8), 3269-3292.

Dziewonski, A.M. and J.H. Woodhouse, (1983), Studies of the seismic source using normal-mode theory, in Kanamori, H. and E. Boschi, eds., Earthquakes: observation, theory, and interpretation: notes from the International School of Physics "Enrico Fermi" (1982: Varenna, Italy), North-Holland Publ. Co., Amsterdam, pp. 45-137.

Ekström, G., (1994), Rapid Earthquake Analysis Utilizes the Internet, *Computers in Physics,* 8: 632-638.

Feigl, K. L., and 14 others, (1993), Space geodetic measurement of crustal deformation in central and southern California, 1984-1992, *J. Geophys. Res.*, 98, 21677-21712.

Freund, L. B., and D. M. Barnett, (1976), A two-dimensional analysis of surface deformation due to dip-slip faulting, *Bull. Seismol. Soc. Am.*, 66, 667-675.

Freymueller, J., S. C. Cohen, and H. J. Fletcher, (2000), Spatial variations in present-day deformation, Kenai Peninsula, Alaska, and their implications, *J. Geophys. Res.*, 105(B4), 8079-8101.

Freymueller, J., C. Zweck, H. Fletcher, S. Hreinsdttir, S.C. Cohen, and M. Wyss, The great Alaska "earthquake" of 1998-2001, (2001), *Eos. Trans. AGU, 82(47), Fall Meeting Supple.*, Abstract G22D-11.

Gilpin, L. M., (1995), Holocene paleoseismicity and coastal tectonics of the Kodiak Islands, Alaska, University of California, Santa Cruz, pp. 357., PhD Thesis.

Gilpin, L.M., G.A. Carver, S. Ward, and R.S. Anderson, (1994), Tidal benchmark readings and postseismic rebound of the Kodiak Islands, SW extent of the 1964 great Alaskan earthquake rupture zone, *Seism. Res. Lett.*, v 65(1), 68.

Hansen, R.A., and N.A. Ratchkovski, (2001), The Kodiak Island, Alaska, M_w 7 earthquake of December 6, 1999, *Seism. Res. Lett.*, 72, 22-32.

Herring, T. A., GLOBK, (2002), Global Kalman filter VLBI and GPS analysis program, Release 10.0, Mass. Inst. of TechnoL,pp. 98, Cambridge.

Holdahl, S. and J. Sauber, (1994), Coseismic slip in the 1964 Prince William Sound earthquake: a new geodetic inversion, *Pageoph.* 142(1), 55-82.

Johnson, J.M., K. Satake, S.R. Holdahl, and J.Sauber, (1996), The 1964 Prince William Sound earthquake, joint inversion of tsunami and geodetic data, *J. Geophys. Res.*, 101, 523-532.

King, R. W. and Y. Bock, (2003), Documentation for the GAMIT GPS analysis software: GAMIT, Mass. Inst. Of TechnoL, version 10.1, Cambridge.

Ma, C., J. M. Sauber, L. J. Bell, T. A. Clark, D. Gordon, W. E. Himwich, and J. W. Ryan, (1990), Measurement of horizontal motions in Alaska using very long baseline interferometry, *J. Geophys. Res.*, 95(B13), 21991-22011.

McCaffrey, R., P.C. Zwick, Y. Bock, L. Prawirodirdjo, J. F. Genrich, C.W. Stevens, S.S.O. Puntodewo, and C. Subarya, (2000), Strain partitioning during oblique plate convergence in northern Sumatra: Geodetic and seismologic constraints and numerical modeling, *J. Geophys. Res.*, 105(B12), 28,363-28,376.

McClusky, S., and 27 authors, (2000), Global Positioning System constraints on plate kinematics and dynamics in the eastern Mediterranean and Caucasus, *J. Geophys. Res.*, 105(B3), 5695-5719.

Melosh, H.J., and A. Raefsky, (1981), A simple and efficient method for introducing faults into finite element computations, *Bull. Seismol. Soc. Am.*, 71, 1391-1400.

Nishenko, S. P., and K.H. Jacob, (1990), Seismic potential of the Queen Charlotte-Alaska-Aleutian seismic zone, *J. Geophys. Res.*, 95(B3), 2511-2532.

Oleskevich, D. A., R. D. Hyndman, and K. Wang, (1999), The updip and downdip limits to great subduction earthquakes: Thermal and structural models of Cascadia, south Alaska, SW Japan, and Chile, *J. Geophys. Res.*, 104(B7), 14965-14991.

Plafker, G., (1969), Tectonics of the March 27, 1964, Alaska earthquake, *U.S. Geological Survey Professional Paper*, 543-I, 74p..

Plafker, G., J. C. Moore, and G. R. Winkler, (1994), Geology of the southern Alaska margin, in The Geology of Alaska Vol. GNA-G-1, G. Plafker and H. C. Berg eds..

Pulpan, H., and C. Frohlich, (1985), Geometry of the subducted plate near Kodiak Island and lower Cook Inlet, Alaska determined from relocated earthquake hypocenters, *Bull. Seismol. Soc. Am.*, 75, 791-810.

Ratchkovski, N.A. and R.A. Hansen, (2001), Sequence of strong intraplate earthquakes in the Kodiak Island region, Alaska, 1999-2001, *Geophys: Res. Lett.*, 28, 3729-3732.

Ryan, J. W., C. Ma, and D. S. Caprette, (1993), NASA space geodesy program, GSFC data analysis- 1992, NASA Tech. Memo, TM-104572.

Sauber, J., T.A. Clark, L.J. Bell, M. Lisowski, C. Ma, D.S. Caprette, (1993), Geodetic measurement of static displacement associated with the 1987—1988 Gulf of Alaska earthquakes, in *Contributions of Space Geodesy to Geodynamics: Crustal Dynamics, Geodynamics 23, AGU,* 233-248.

Sauber, J., S. Stockman, and T. Clark, (1998), Educational outreach strategy involves K-12 students in earthquake hazard research, *Eos, Trans., AGU,* 79(33), 393,396-397.

Sauber, J., G. Plafker, B.F. Molnia, and M. A. Bryant, (2000), Crustal deformation associated with glacial fluctuations in the eastern Chugach Mountains, Alaska, *J. Geophys. Res.,* 105(B4), 8055-8077.

Savage, J. C., (1983), A dislocation model of strain accumulation and release at a subduction zone, *J. Geophys. Res.,* 88, 4984-4996.

Savage, J.C. and G. Plafker, (1991), Tide gage measurements of uplift along the south coast of Alaska, *J. Geophys. Res.,* 96, 4325-4335.

Savage, J.C., J.L. Svarc, and W. H. Prescott, (1999), Deformation across the Alaska-Aleutian Subduction Zone near Kodiak, *Geophys. Res. Lett.,* 26, 2117-2120.

Scholz, C., (1990), The mechanics of earthquakes and faulting, 437 p., Cambridge University Press, Cambridge.

Stockman, S., J. Sauber, and E. Linscheid, (1997), A High School and NASA join forces to investigate the Alaska-Aleutian subduction zone near Kodiak Island, *J. Geoscience Education,* 45, 440-446.

Taylor, M. A. J., G. Zheng, J. R. Rice, W. D. Stuart, R. Dmowska, (1996), Cyclic stressing and seismicity at strongly coupled subduction zones, *J. Geophys. Res.,* 101(B4)}, 8363-8381.

vonHuene, R., D. Klaeschen, and J. Fruehn, (1999), Relation between the subducting plate and seismicity associated with the great 1964 Alaska earthquake, in Seismogenic and Tsunamigenic Processes in Shallow Subduction Zones, J. Sauber and R. Dmowska, eds., *PAGEOPH, 154(3-4).*

Wahr, J., and M. Wyss, (1980), Interpretation of postseismic deformation with a viscoelastic relaxation model, *J. Geophys. Res.,* 85, 6471-6477.

Wells, R. E., R. J. Blakely, Y. Sugiyama, D.W. Scholl, P.A. Dinterman, (2003), Basin centered asperities in great subduction zone earthquakes: a link between slip, subsidence, and subduction erosion?, *J. Geophys. Res.*, 108(B10), 2002JB002072.

Zheng, G., R. Dmowska, J. R. Rice, (1996), Modeling earthquake cycles in the Shumagin subduction segment, Alaska, with seismic and geodetic constraints, *J. Geophys. Res.*, 101(B4), 8383-8392.

Zweck, C., J. T. Freymueller, and S.C. Cohen, (2002), Three-dimensional elastic dislocation modeling of the postseismic response to the 1964 Alaska earthquake, *J. Geophys. Res.*, 107(B4), 10.1029/2001JB000409.

Figure Captions

Figure 1. Geologic map of Kodiak Islands region of Alaska (modified from H. M. Beikman 1980). The location of the northern Kodiak stations are given by circles and the southern Kodiak Island stations in the Katmai network of *Savage et al.* [1999] are given by squares. The location of Kodiak Island (KI) on an outline of the state of Alaska is given in the upper right hand corner. The scale on the lower right is given in kilometers. Region I: Eastern coastal regions includes Narrow Cape fold and thrust belt, the Narrow Cape fault, and along the western boundary of Region I, the Kodiak Island fault. Brown (IT) = Lower Tertiary Ghost Rock Formation, lt Tan(Tm) = Miocene Rocks, Narrow Cape formation, Yellow (To) = Oligocene stratified sedimentary sequence; Region II: Late Cretaceous Belt. This central region appears to have uplifted more rapidly than the region northwest of the Border Ranges fault resulting in a northwest tilt of the Islands [*Gilpin* ,1995], bright Green (uK) = upper Cretaceous stratified sedimentary sequence, Kodiak formation, Pink (Txif) = Paleocene felsic, intrusive rocks, Kodiak Batholith; Region III: This region of volcanic arc basement forms a backstop northwest of the Border Ranges fault (BR), Green (Kj3) = Lower Cretaceous and Upper Jurassic rocks, Uyak formation, Maroon(u)=Precambrian ultramafic, Turquoise,(uTr) = Triassic volcanics, Shuyak formation, Pink with white (Jii)= Jurassic Blueschist-Greenschist, Raspberry Schist. BR = Border Ranges fault. The degree of lithification generally increases from southeast to northwest across the Island [*Gilpin*, 1995].

Figure 2. Map showing representative GPS station velocities from the northern Kodiak network (Table 1) and the southern Kodiak Island stations from the Katmai network [*Savage et al.*, 1999] with our computed horizontal velocity and 95% confidence error ellipses (in red). Focal mechanisms derived from Harvard Centroid Moment Tensor and USGS Fast Moment Tensor

solutions (1977-2004, *Dziewonski and Woodhouse* 1983; *Ekstrom,* 1994; http://neic.usgs.gov/neis/sopar) were plotted using the program iGMT [*Becker and Braun,* 1998]. The event location, fault plane parameters, and date are given in Table 5. Note: The longitude is given in °E.

Figure 3. The detrended north, east, and vertical time series of station position for stations from the Kodiak GPS northern and southern networks that have been observed at least 3 times.

Figure 4. The station velocities resolved into trench-normal and trench-parallel components as a function of distance from the trench (taken to be from the southeastern most extent of the 4000 or 5800 m bathymetry contour). The error bars are two-sigma. The station names are indicated along the top of the graph, the black data points are from northern Kodiak and southern Kodiak stations are given in red. Positive velocities for the trench normal component indicate away from the trench. Negative velocities for the trench parallel component indicate a west directed velocity.

Figure 5 (a) Two dimensional finite element grid used in MD1 and MD2 models (modified from *Cohen* [1996], with the details of the model geometry given in Table 3 in that reference). The "zero slab depth" location in our finite element and dislocation models is seaward (primarily east) of the trench and corresponds to the projection of the slab to the surface. A low viscosity zone occurs below a depth of 38 km in MD1 and below 90 km in the MD2 models. In our reference model a viscosity of 5×10^{19} Pa s is assumed; this corresponds to a Maxwell time, τ, equal to 26 years; this is short relative to the estimated repeat time of major earthquakes in the northern Kodiak region of 300-500 years [*Gilpin,* 1995]. The dark line between the downgoing Pacific plate (in red) and the overriding continental plate (in green) represents the region of reduced slip during the 1964 earthquake and partial locking during the interseismic time interval

in some models. Within the "Key" are the assumed elastic parameters (E) and viscosity μ for the reference model.

b. Coseismic slip (meters) in the 1964 earthquake as a function of depth for the MD1 (solid line) and MD2 (dashed line) models. The MD2 model includes reduced slip between 22 and 90.

c. Input slip (mm/yr) for interseismic time period as a function of depth for Elastic (dotted), MD1a (dashed) and MD1b (solid line).

d. Input slip (mm/yr) for interseismic time period as a function of depth for MD2a (dashed), MD2b (dotted), and MD2c (solid) and MD2d (dash-dot).

Figure 6. Predicted coseismic vertical displacement as a function of distance for the two slip models in Figure 5b along with coseismic data (asterick with error bar for the north and diamond with error bar in red for the south) from *Plafker* [1969]. Model 1 (MD1) is given by a solid line and Model 2 (MD2) by a dotted line, in black for northern Kodiak and in red for southern Kodiak. The coseismic data of *Plafker* [1969] given here corresponds to a time interval of up to 14 months (see text). The down-dip slip in MD2 between 22 and 90 km is assumed to represent a longer post-seismic time interval.

Figure 7. (a) Comparison of the geodetically estimated rate of deformation (trench normal) to the predicted horizontal velocity from the Elastic (dotted, *Savage et al.*, [1999]) and the MD1a (solid), MD1a(solid red) for southern Kodiak and MD1b (dashed) viscoelastic models. The northern Kodiak trench-normal data is given in black and the southern Kodiak data in red. Note that none of these models predict trench directed velocities at distances of ~300-400 km (Alaska Peninsula). (b) same models as given in a. but for the vertical displacement rate as a function of distance from the trench. The vertical uplift rate at KRLK is not matched by any of the models.

Figure 8. (a) Comparison of the predicted horizontal velocities for the four MD2 models of Table 4, plus southern Kodiak for the preferred model of MD2c (red), to the observed horizontal velocities, (b) the observed versus vertical displacement rate for the four MD2 models, plus southern Kodiak model of MD2c (red), (c) the observed versus predicted horizontal velocities for the MD2c model including the individual elements (dotted=interseismic, dashed=postseismic, and dash-dot=creep) and all three components together (total solid line). Data description as given in Figure 7. And (d) the predicted horizontal velocity for the MD2c model assuming four different viscosities 10^{19}, 5×10^{19}, 10^{20} and 5×10^{20} Pa s and for southern Kodiak MD2c (solid red) for a viscosity of 5×10^{19} Pa s.

Figure 9. Comparison of the predicted vertical displacement between 1965 and 1993 assuming the model parameters for MD2b (dashed line), MD2c (solid line), MD2c (solid red) over a 28 year time period compared to the temporary tide gauge data of *Gilpin* [1995]. The higher creep rate model of MD2b better matches the uplift rate observed 1965-1993.

Table 1. Site Location and Observation History

Station	Abbreviation	Latitude,°N	Longitude,°W (°E)	1993[a]	1995[a]	1997[a]	1998[a]	1999[a]	2000[a]	2001[a]	2002[a]	2003[a]
Sitkink*	SITK	56.54	-154.14(205.86)	3	2	4	0	0	0	0	0	0
Pasagshak	PASA	57.44	-152.46(207.54)	0	0	3	0	2	0	1	0	0
Eastern Coast–Kodiak DGPS Site, KOD1, and Extended footprint												
Kodiak DGPS	KOD1	57.62	-152.19(207.81)	0	0	27	3	7	10	6	6	5
Chiniak	CHIN	57.62	-152.16(207.84)	0	3^T	1^T	0	0	0	0	0	0
Miller FieldA	MILA	57.61	-152.20(207.80)	0	1^T	0	0	0	0	0	0	0
Miller FieldB	MILB	57.62	-152.19(207.81)	0	2^T	1^T	2	3	0	0	0	0
Akhiok*	AHKI	57.94	-154.17(205.83)	4	1	3	0	0	0	0	0	0
Clam	CLAM	57.65	-152.51(207.49)	0	3^T	2	0	3	1	0	0	0
Kodiak Fiducial and Extended Footprint Near Town of Kodiak												
Kodiak RM2	KODI	57.74	-152.50(207.50)	13^+	27^+	4^+	3^+	6^+	1	1	0	0
Kodiak IGS	KODK	57.73	-152.50(207.50)	0	0	0	0	0	10	11	6	0
Kodiak VLBI	KODV	57.74	-152.50(207.50)	1	1^T	0	0	0	0	0	0	0
NOAA Vertical	NOAA	57.73	-152.50(207.50)	0	0	0	0	0	2	0	0	0
Ski Challet	SKI0	57.80	-152.61(207.39)	0	4^T	1^T	0	2	0	2	0	0
Karluk*	KRLK	57.56	-154.45(205.55)	3	2	3	5	0	0	0	0	0

[a]Number of observation days; KODK, KOD1, 24 hrs; KODI, AHKI, SITK, KARL, 7-24 hrs, others 3-8 hrs
[T]Trimble L1/L2 antenna; otherwise choke ring antenna
[+]Spike mount; otherwise tripod set-up
*Katmai network of Savage et al., 1999

Table 2. North America fixed reference frame stations.

Station	North Rate (mm/yr)	N_σ (mm/yr)	East Rate (mm/yr)	E_σ (mm/yr)	Vertical (mm/yr)	V_σ (mm/yr)
North American stations						
STJO	0.82	0.86	-0.22	0.87	-0.28	0.87
BRMU	0.70	0.62	0.15	0.63	-1.42	0.85
ALGO	-0.33	0.63	0.25	0.64	2.98	0.73
NLIB	0.50	0.32	0.53	0.34	-1.14	0.82
MDO1	0.11	0.30	-0.37	0.33	0.23	0.82
PIE1	-0.25	0.78	-0.26	0.80	2.08	0.80
YELL	-0.44	0.25	0.38	0.25	3.86	1.13
WILL	0.78	0.98	-0.08	1.00	-0.08	1.27
Pacific Plate Stations						
CHAT	52.87	0.89	-38.22	0.88	1.14	1.30
KWJ1	47.17	1.13	-69.44	1.33	-3.76	2.86
MKEA	51.62	0.87	-59.75	0.91	-2.67	2.83

Note: The correlation between components is less than 0.03.

Table 3. Site Velocities in a North American reference frame and their plate-parallel(N22°W), plate-normal(N68°W), trench-normal(N30°W), and trench-parallel (N60°W) components.

Site Name	Distance, from Trench(km)	Horizontal Rate, (mm/yr) ± 1σ	Orientation, (°)± 1σ	Vertical, (mm/yr) ± 1σ	N22°W Rate(mm/yr)	N68°W Rate(mm/yr)	N30°W Rate(mm/yr)	N60°E Rate(mm/yr)
SITK*	120.	29.7±1.7	N30.3W±3.3	-2 ±4	29.4	-4.3	29.7	-0.2
PASA	147.	25.3±1.4	N32.9W±4.2	8 ±10	24.8	-4.8	25.3	-1.3
KOD1	153.	17.6±2.1	N28.8W±6.8	6 ±2	17.5	-2.1	17.6	0.4
MILB	153.	18.5±1.8	N20.8W±5.5	16 ±5	18.5	0.4	18.3	2.9
AHKI*	159.	19.1±2.2	N33.5W±6.6	2 ±5	18.7	-3.8	19.1	-1.2
CLAM	172.	14.0±1.3	N39.5W±5.5	17 ±3	13.4	-4.2	13.8	-2.3
KODI	182.	11.3±1.5	N49.3W±7.7	14 ±4	10.0	-5.2	10.6	-3.7
KODK	182.	13.5±1.6	N48.3W±6.7	9 ±5	12.1	-5.9	12.8	-4.2
SKI0	192.	8.5±1.0	N59.7W±6.5	12 ±3	6.7	-5.2	7.4	-4.2
KRLK*	228.	8.0±1.3	N62.4W±9.3	19 ±4	6.1	-5.2	6.7	-4.3
				Predicted Pacific Plate Motion Relative to Stable North America				
Nuvel-1A					57.	0.0	56.4	-7.9

*Katmai network of Savage et al., 1999

Table 4. Interseismic Model Parameters

Model Number	Coseismic Model	Depth of Low Viscosity	Interseismic Locked Zone	Creep Region, Rate (mm/yr)
Elastic	None	None	5≤z km≤ 18	None
MD1a	9-11≤z km≤22-30	38	9-11≤z km≤22-30	None
MD1b	9-11≤z km≤22-30	38	5-12≤z km≤17-22	None
MD2a	dotted line in Fig. 6b	90	dash + solid	10
MD2b	dotted line in Fig. 6b	90	dash-dot	25
MD2c	dotted line in Fig. 6b	90	solid line	10
MD2d	dotted line in Fig. 6b	90	dot + dash-dot	25

Table 5 Event locations, fault plane parameters, and date.

Event Num.	Lon (°E)	Lat (°N)	Str1	Dip1	Rake1	Str2	Dip2	Rake2	Date (MMDDYR)
1	-154.43	58.09	42	65	22	302	70	153	112777
2	-151.21	56.30	265	8	119	55	83	86	071978
3	-154.16	56.20	244	13	94	60	77	89	070680
4	-151.38	56.91	215	9	78	47	82	92	090682
5	-155.43	56.95	85	59	-18	185	75	-147	112683
6	-154.18	58.62	334	25	-164	229	83	-65	032384
7	-154.06	58.58	319	50	168	56	81	41	102785
8	-153.38	56.11	220	18	75	56	73	95	030686
9	-153.20	58.88	89	64	12	353	80	153	052386
10	-153.21	56.06	241	11	105	46	79	87	091686
11	-152.28	56.30	228	8	85	53	82	91	052087
12	-154.64	57.70	319	28	-176	225	88	-62	061689
13	-153.17	58.30	176	62	-154	73	67	-31	030890
14	-153.09	56.89	212	9	61	62	82	94	052990
15	-155.48	56.34	0	70	173	93	84	20	080192
16	-154.87	57.24	358	29	-148	239	75	-65	091292
17	-153.81	56.80	61	33	-67	214	60	-105	042293
18	-149.96	58.49	141	23	-150	23	79	-70	121594
19	-152.83	57.03	58	4	-66	214	87	-91	030396
20	-151.54	56.14	218	20	60	70	72	101	120896
21	-152.07	56.73	299	5	159	50	88	85	110898
22	-152.86	56.48	209	11	101	18	79	88	050699
23	-152.58	56.21	225	9	74	61	81	93	050799
24	-154.78	58.15	64	49	-17	165	78	-138	082699
25	-154.35	57.35	357	63	-180	267	90	-27	120699
26	-154.38	57.22	350	37	-161	245	79	-55	120799
27	-154.04	57.24	5	75	178	96	88	15	011600
28	-149.29	57.47	302	55	136	61	55	45	012300
29	-154.44	57.41	350	10	-139	219	84	-83	030800
~~30~~	~~-154.28~~	~~57.48~~	~~26~~	~~15~~	~~-96~~	~~212~~	~~75~~	~~-88~~	~~050800~~
31	-152.84	58.97	330	56	-174	236	85	-35	051900
32	-150.18	58.65	82	63	24	341	69	150	062800
33	-154.22	57.54	356	47	-161	253	76	-44	071100
34	-154.24	57.58	224	42	-36	341	67	-127	091900
35	-153.70	58.00	98	60	35	349	60	145	092500
36	-153.56	56.99	224	8	74	60	82	92	011001
37	-153.63	56.51	225	7	92	43	83	90	021101
38	-150.99	57.06	332	66	170	66	81	24	071901
39	-154.97	58.82	63	64	26	321	67	151	072801
40	-155.11	57.63	278	35	73	119	57	102	082901
41	-151.26	58.50	218	32	-31	335	74	-118	090502
42	-151.44	58.33	154	8	-14	258	88	-98	012004

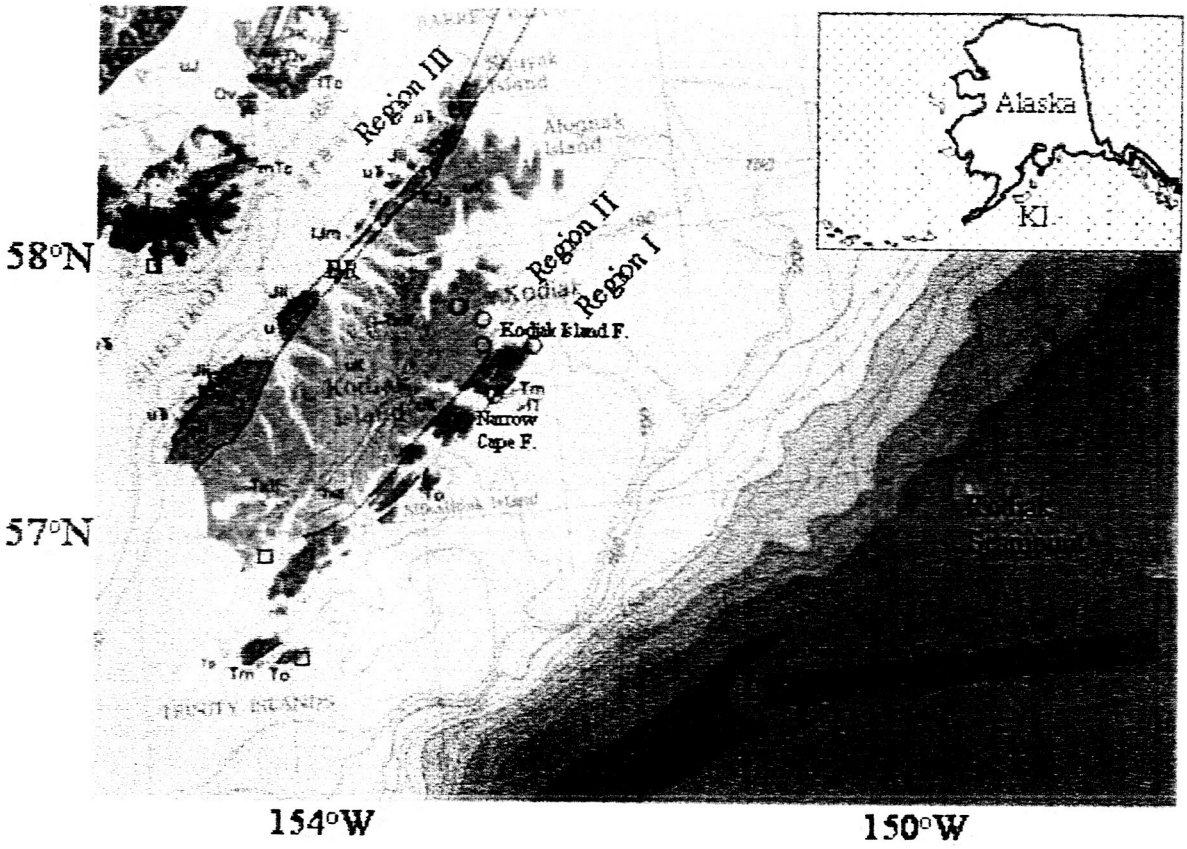
Region III
Region II
Region I
Alaska
KI
58°N
57°N
Kodiak Island F.
Narrow
Cape F.
Tm
To
154°W
150°W

Figure 1

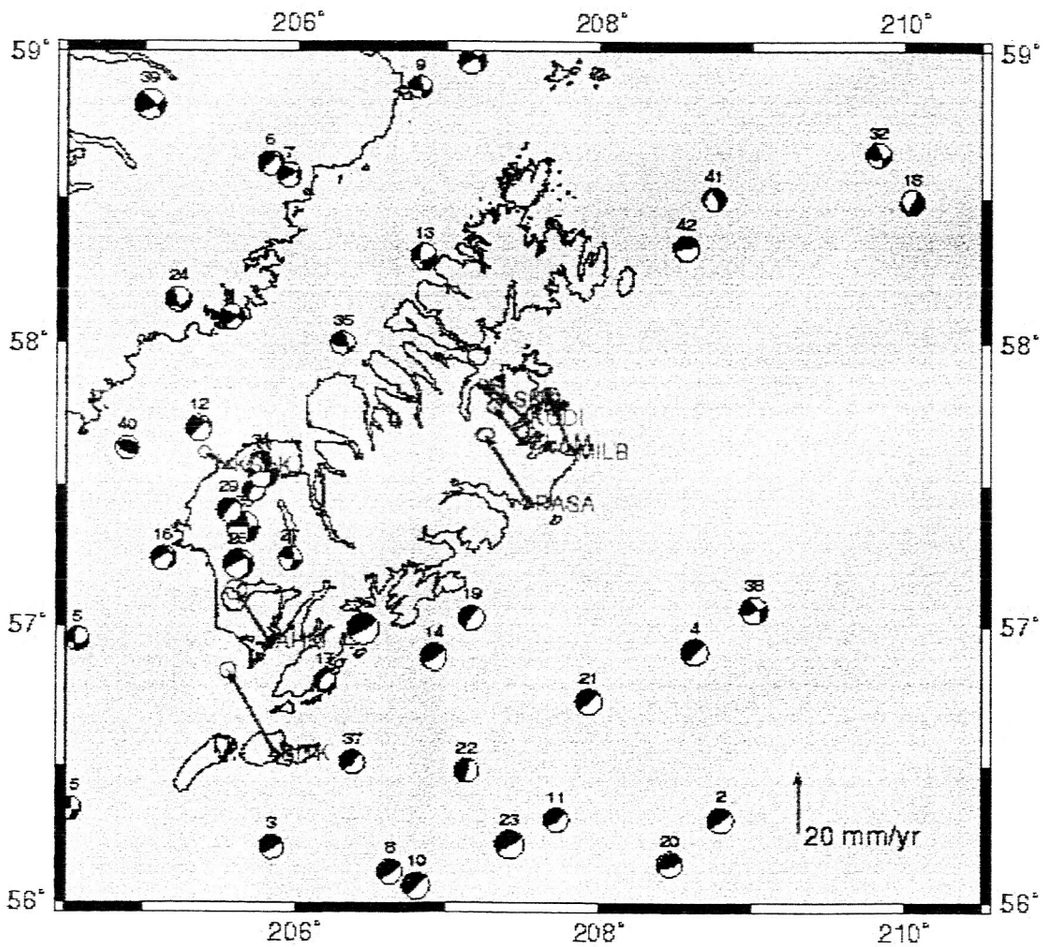

Figure 2

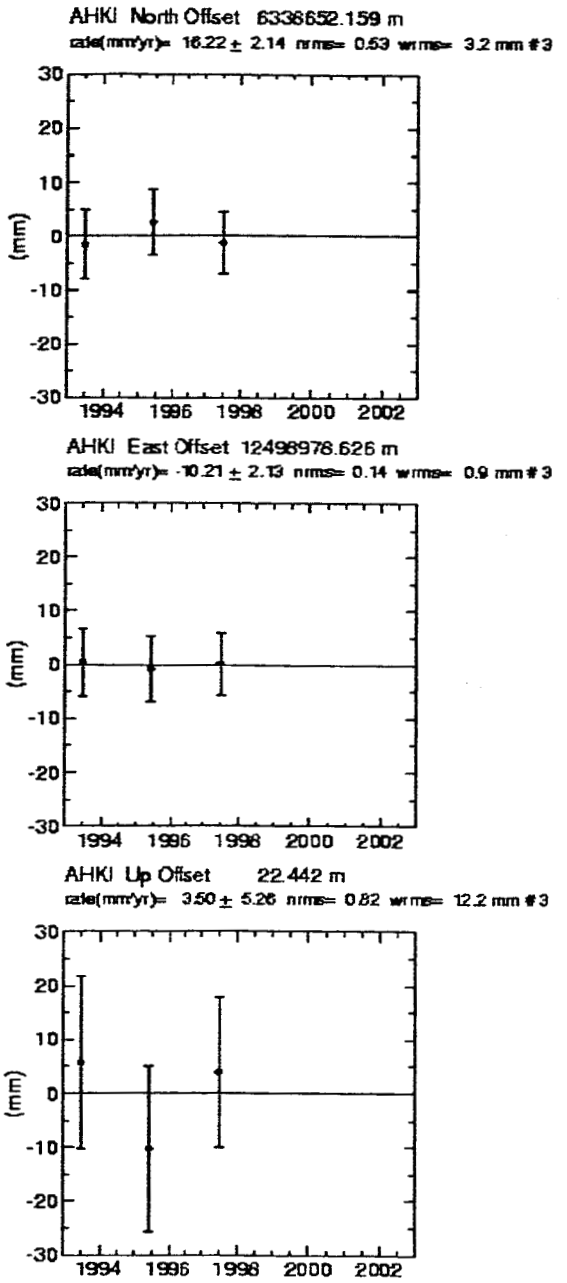
AHKI North Offset 6336652.159 m
rate(mm/yr)= 16.22 ± 2.14 nrms= 0.53 wrms= 3.2 mm #3
AHKI East Offset 12498978.626 m
rate(mm/yr)= -10.21 ± 2.13 nrms= 0.14 wrms= 0.9 mm #3
AHKI Up Offset 22.442 m
rate(mm/yr)= 3.50 ± 5.26 nrms= 0.82 wrms= 12.2 mm #3
(mm)
30
20
10
0
-10
-20
-30
1994
1996
1998
2000
2002

Figure 3a

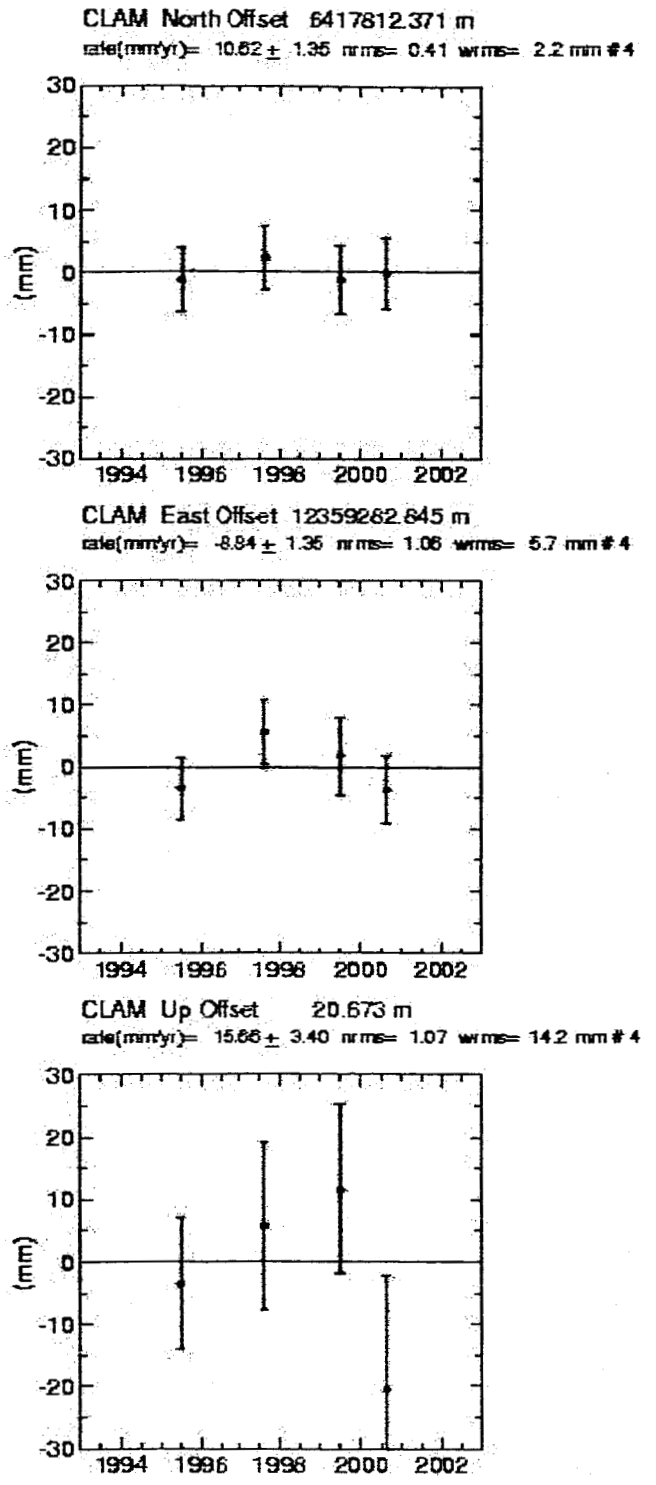
CLAM North Offset 6417812.371 m
rate(mm/yr)= 10.62 ± 1.35 nrms= 0.41 wrms= 2.2 mm # 4
30
20
10
0
-10
-20
-30
(mm)
1994
1996
1998
2000
2002
CLAM East Offset 12359282.845 m
rate(mm/yr)= -8.84 ± 1.35 nrms= 1.06 wrms= 5.7 mm # 4
30
20
10
0
-10
-20
-30
(mm)
1994
1996
1998
2000
2002
CLAM Up Offset 20.673 m
rate(mm/yr)= 15.66 ± 3.40 nrms= 1.07 wrms= 14.2 mm # 4
30
20
10
0
-10
-20
-30
(mm)
1994
1996
1998
2000
2002

Figure 3b

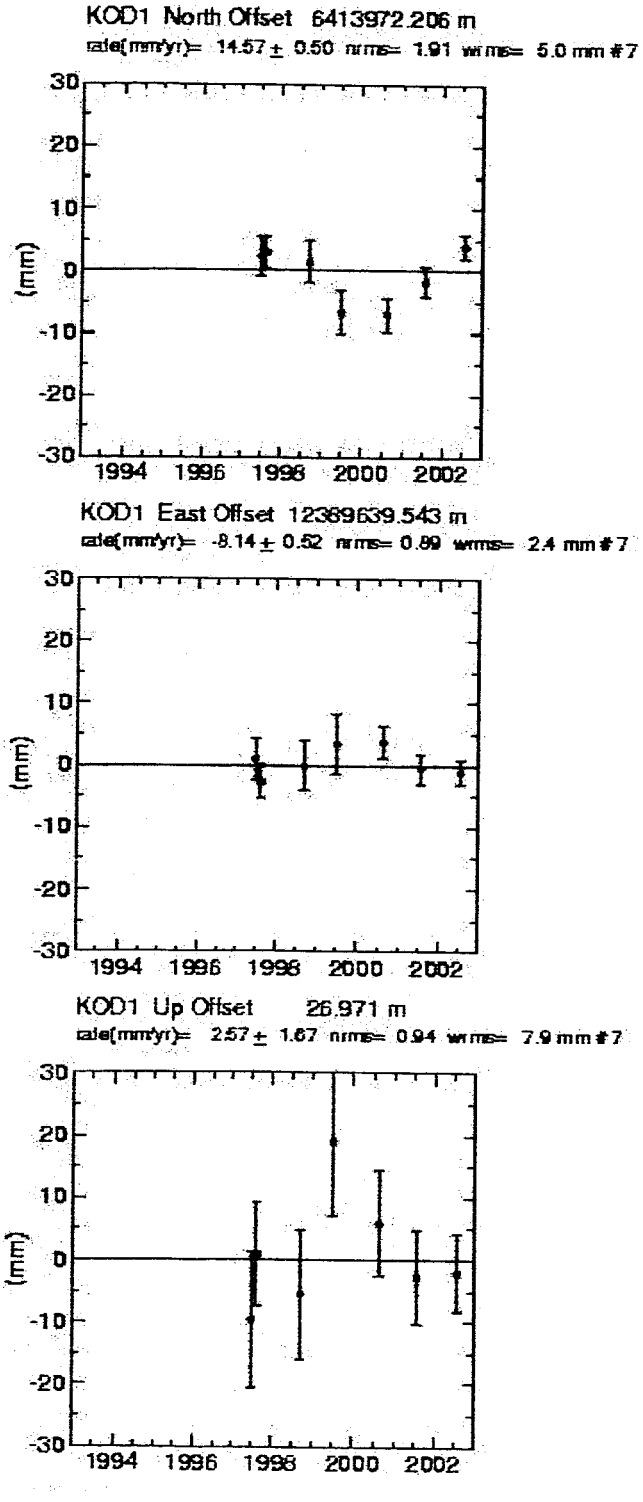
KOD1 North Offset 6413972.206 m
rate(mm/yr)= 14.57 ± 0.50 nrms= 1.91 wrms= 5.0 mm #7
KOD1 East Offset 12389639.543 m
rate(mm/yr)= -8.14 ± 0.52 nrms= 0.89 wrms= 2.4 mm #7
KOD1 Up Offset 26.971 m
rate(mm/yr)= 2.57 ± 1.67 nrms= 0.94 wrms= 7.9 mm #7
(mm)
30
20
10
0
-10
-20
-30
1994
1996
1998
2000
2002

Figure 3c

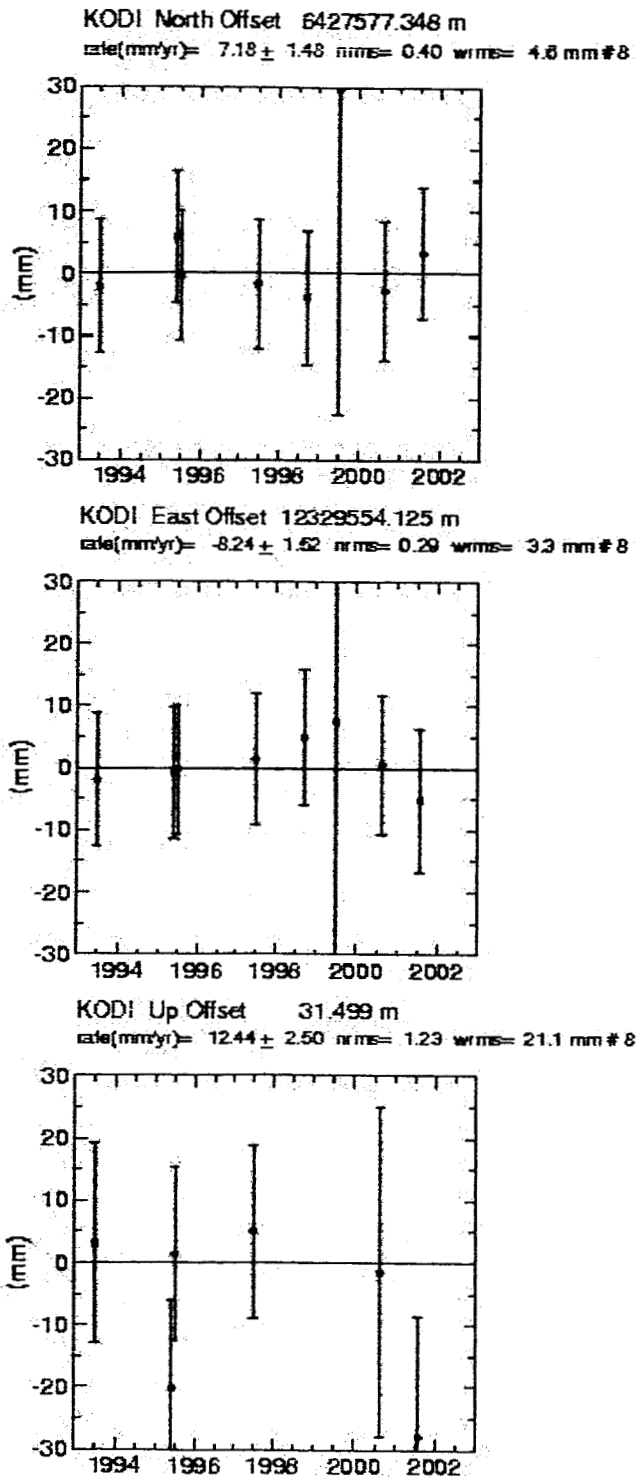
KODI North Offset 6427577.348 m
rate(mm/yr)= 7.18 ± 1.48 nrms= 0.40 wrms= 4.6 mm # 8
(mm)
30
20
10
0
-10
-20
-30
1994
1996
1998
2000
2002
KODI East Offset 12329554.125 m
rate(mm/yr)= -8.24 ± 1.52 nrms= 0.29 wrms= 3.3 mm # 8
(mm)
30
20
10
0
-10
-20
-30
1994
1996
1998
2000
2002
KODI Up Offset 31.499 m
rate(mm/yr)= 12.44 ± 2.50 nrms= 1.23 wrms= 21.1 mm # 8
(mm)
30
20
10
0
-10
-20
-30
1994
1996
1998
2000
2002

Figure 3d

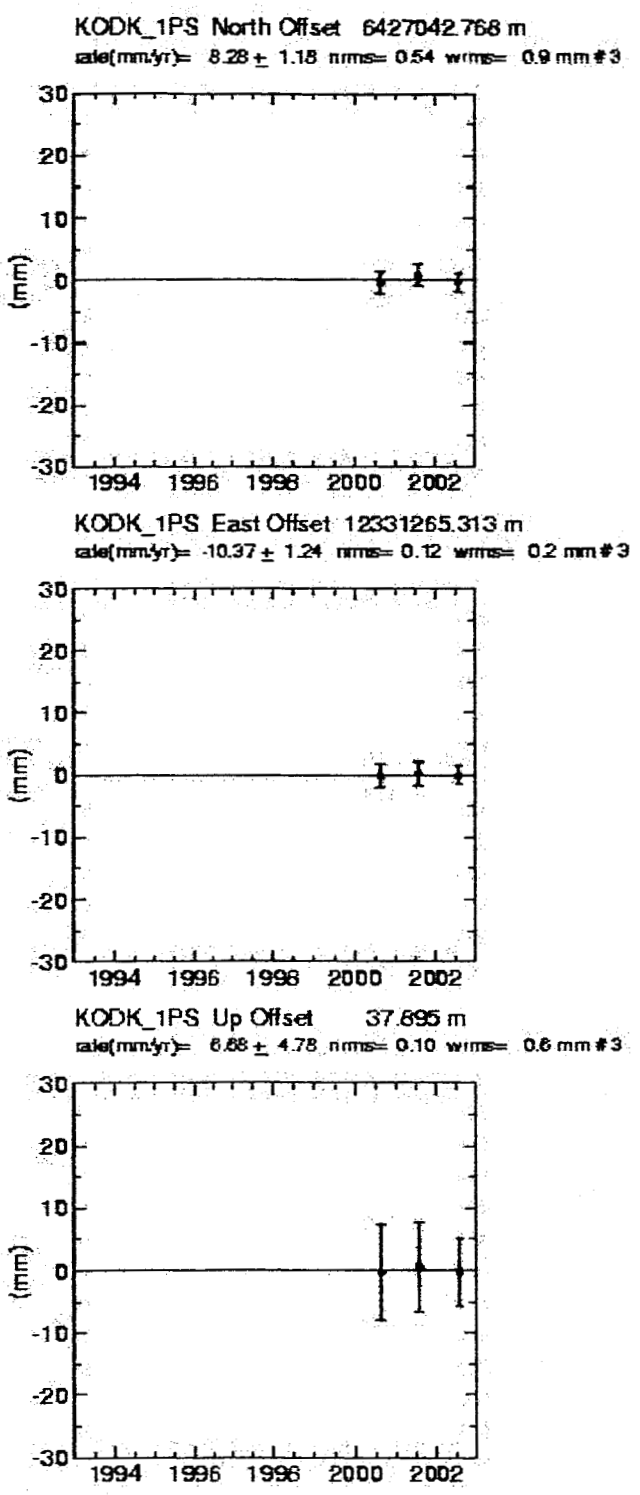
KODK_1PS North Offset 6427042.768 m
rate(mm/yr)= 8.28 ± 1.18 nrms= 0.54 wrms= 0.9 mm # 3
KODK_1PS East Offset 12331265.313 m
rate(mm/yr)= -10.37 ± 1.24 nrms= 0.12 wrms= 0.2 mm # 3
KODK_1PS Up Offset 37.695 m
rate(mm/yr)= 6.68 ± 4.78 nrms= 0.10 wrms= 0.6 mm # 3
(mm)
30
20
10
0
-10
-20
-30
1994
1996
1998
2000
2002

Figure 3e

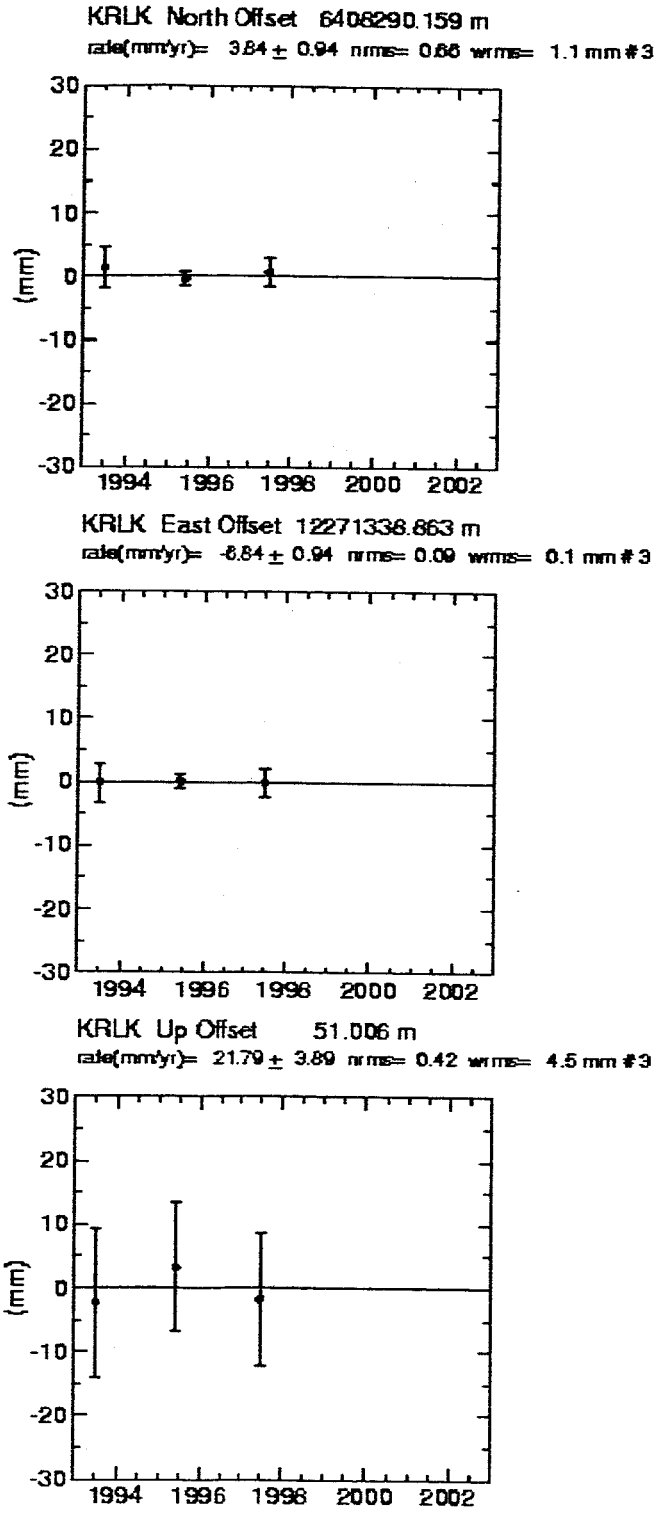
KRLK North Offset 6408290.159 m
rate(mm/yr)= 3.84 ± 0.94 nrms= 0.66 wrms= 1.1 mm # 3
KRLK East Offset 12271338.863 m
rate(mm/yr)= -6.84 ± 0.94 nrms= 0.09 wrms= 0.1 mm # 3
KRLK Up Offset 51.006 m
rate(mm/yr)= 21.79 ± 3.89 nrms= 0.42 wrms= 4.5 mm # 3
(mm)
30
20
10
0
-10
-20
-30
1994
1996
1998
2000
2002

Figure 3f

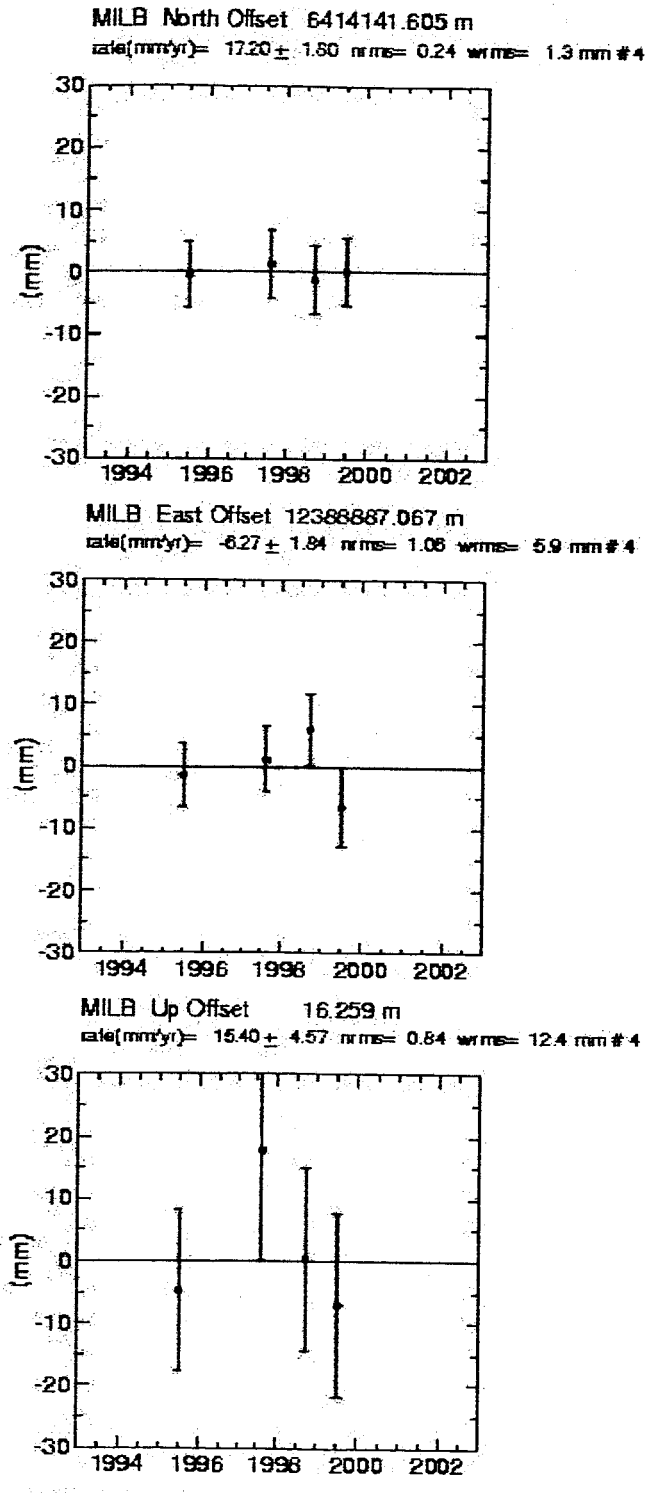
MILB North Offset 6414141.605 m
rate(mm/yr)= 17.20 ± 1.60 nrms= 0.24 wrms= 1.3 mm # 4
30
20
10
0
-10
-20
-30
(mm)
1994 1996 1998 2000 2002
MILB East Offset 12388887.067 m
rate(mm/yr)= -6.27 ± 1.84 nrms= 1.06 wrms= 5.9 mm # 4
30
20
10
0
-10
-20
-30
(mm)
1994 1996 1998 2000 2002
MILB Up Offset 16.259 m
rate(mm/yr)= 15.40 ± 4.57 nrms= 0.84 wrms= 12.4 mm # 4
30
20
10
0
-10
-20
-30
(mm)
1994 1996 1998 2000 2002

Figure 3g

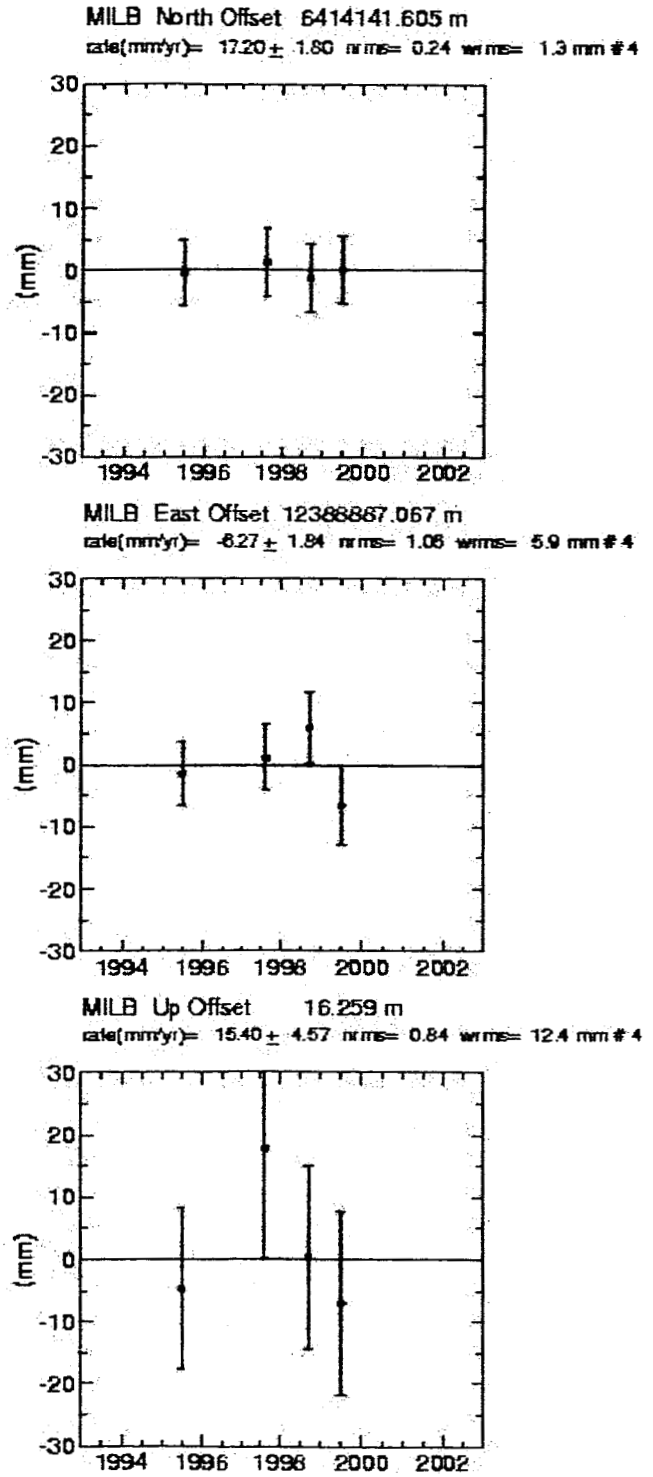
MILB North Offset 6414141.605 m
rate(mm/yr)= 17.20 ± 1.80 nrms= 0.24 wrms= 1.3 mm # 4
MILB East Offset 12388867.067 m
rate(mm/yr)= -6.27 ± 1.84 nrms= 1.06 wrms= 5.9 mm # 4
MILB Up Offset 16.259 m
rate(mm/yr)= 15.40 ± 4.57 nrms= 0.84 wrms= 12.4 mm # 4
(mm)
30
20
10
0
-10
-20
-30
1994
1996
1998
2000
2002

Figure 3g

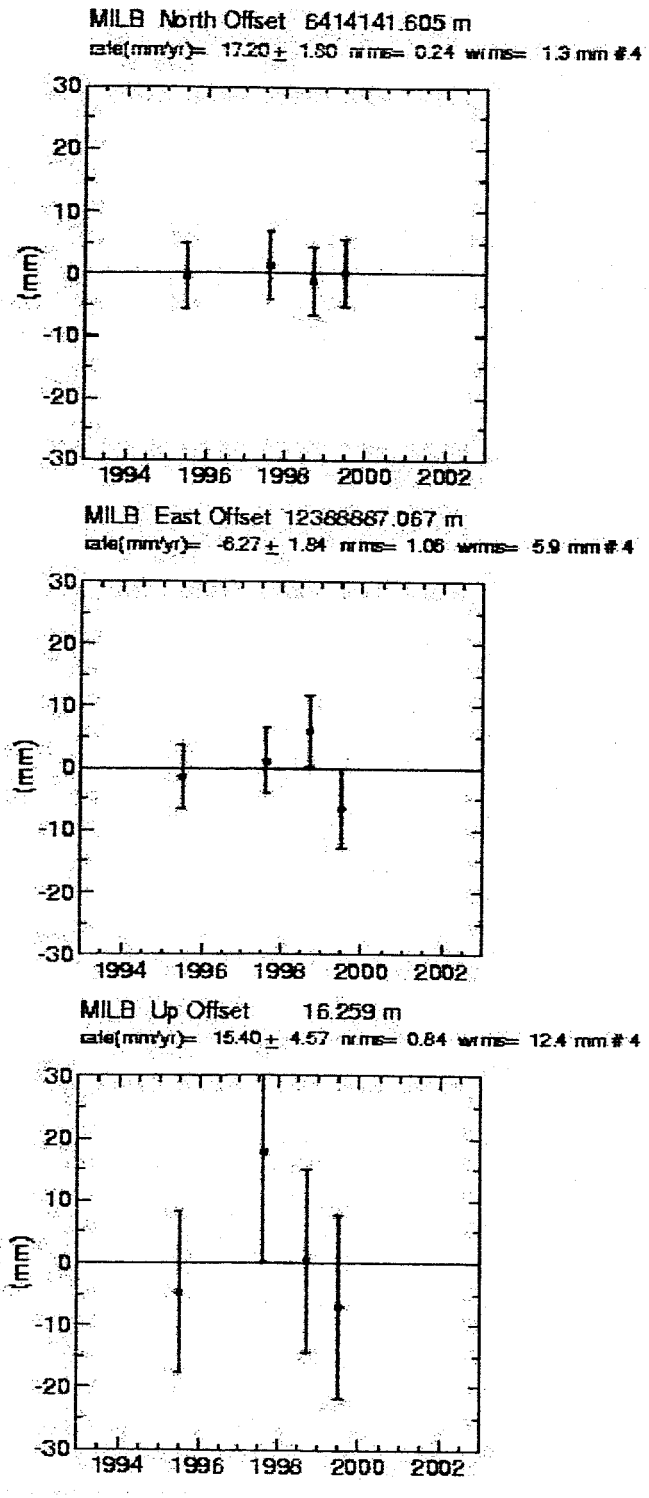
MILB North Offset 6414141.605 m
rate(mm/yr)= 17.20 ± 1.80 nrms= 0.24 wrms= 1.3 mm # 4
30
20
10
0
-10
-20
-30
(mm)
1994 1996 1998 2000 2002
MILB East Offset 12388887.067 m
rate(mm/yr)= -6.27 ± 1.84 nrms= 1.06 wrms= 5.9 mm # 4
30
20
10
0
-10
-20
-30
(mm)
1994 1996 1998 2000 2002
MILB Up Offset 16.259 m
rate(mm/yr)= 15.40 ± 4.57 nrms= 0.84 wrms= 12.4 mm # 4
30
20
10
0
-10
-20
-30
(mm)
1994 1996 1998 2000 2002

Figure 3g

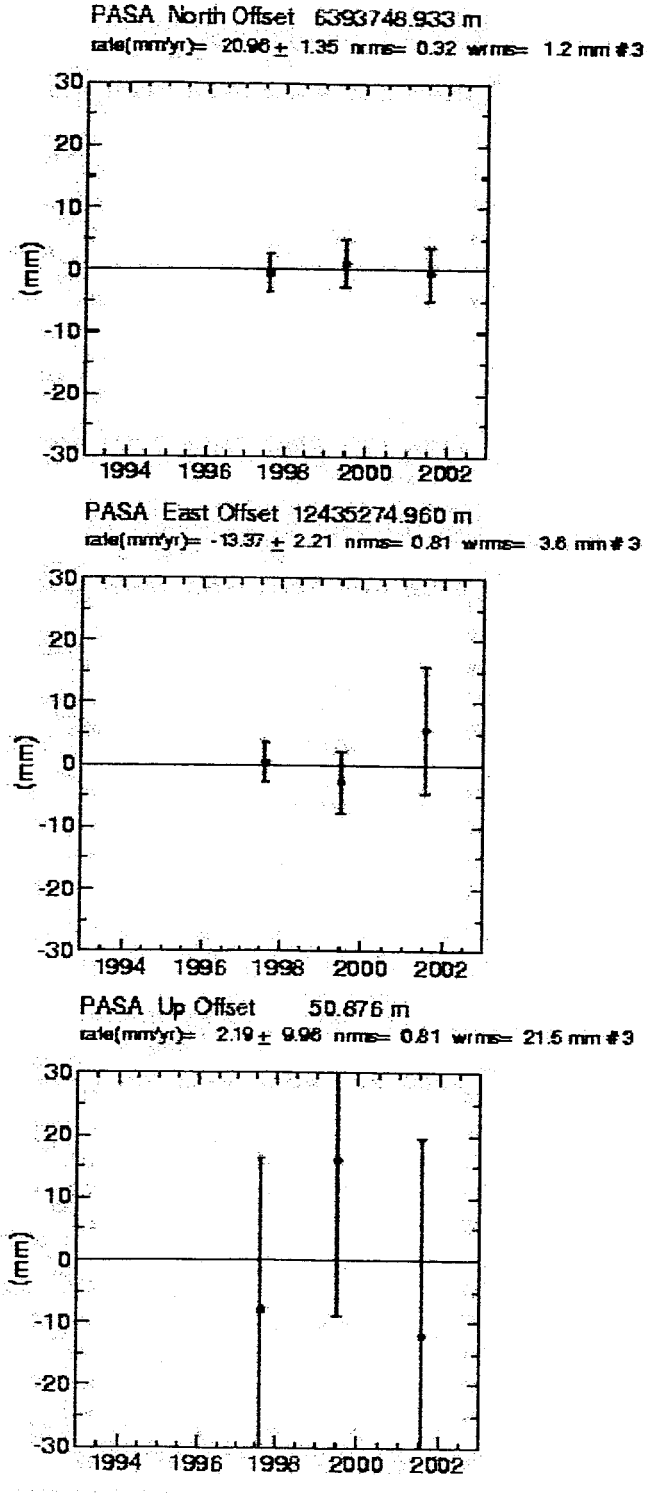
PASA North Offset 6393748.933 m
rate(mm/yr)= 20.96 ± 1.35 nrms= 0.32 wrms= 1.2 mm #3
30
20
10
0
-10
-20
-30
(mm)
1994 1996 1998 2000 2002
PASA East Offset 12435274.960 m
rate(mm/yr)= -13.37 ± 2.21 nrms= 0.81 wrms= 3.6 mm #3
30
20
10
0
-10
-20
-30
(mm)
1994 1996 1998 2000 2002
PASA Up Offset 50.876 m
rate(mm/yr)= 2.19 ± 9.96 nrms= 0.81 wrms= 21.5 mm #3
30
20
10
0
-10
-20
-30
(mm)
1994 1996 1998 2000 2002

Figure 3h

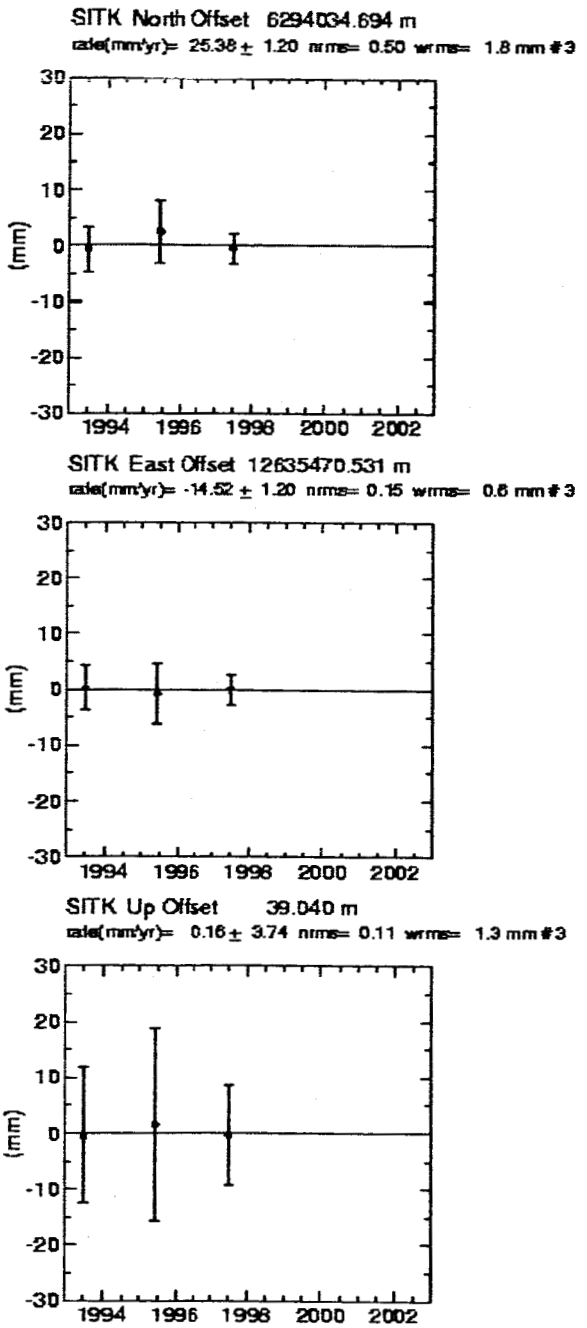
SITK North Offset 6294034.694 m
rate(mm/yr)= 25.38 ± 1.20 nrms= 0.50 wrms= 1.8 mm # 3
30
20
10
0
-10
-20
-30
(mm)
1994
1996
1998
2000
2002
SITK East Offset 12635470.531 m
rate(mm/yr)= -14.52 ± 1.20 nrms= 0.15 wrms= 0.6 mm # 3
30
20
10
0
-10
-20
-30
(mm)
1994
1996
1998
2000
2002
SITK Up Offset 39.040 m
rate(mm/yr)= 0.16 ± 3.74 nrms= 0.11 wrms= 1.3 mm # 3
30
20
10
0
-10
-20
-30
(mm)
1994
1996
1998
2000
2002

Figure 3i

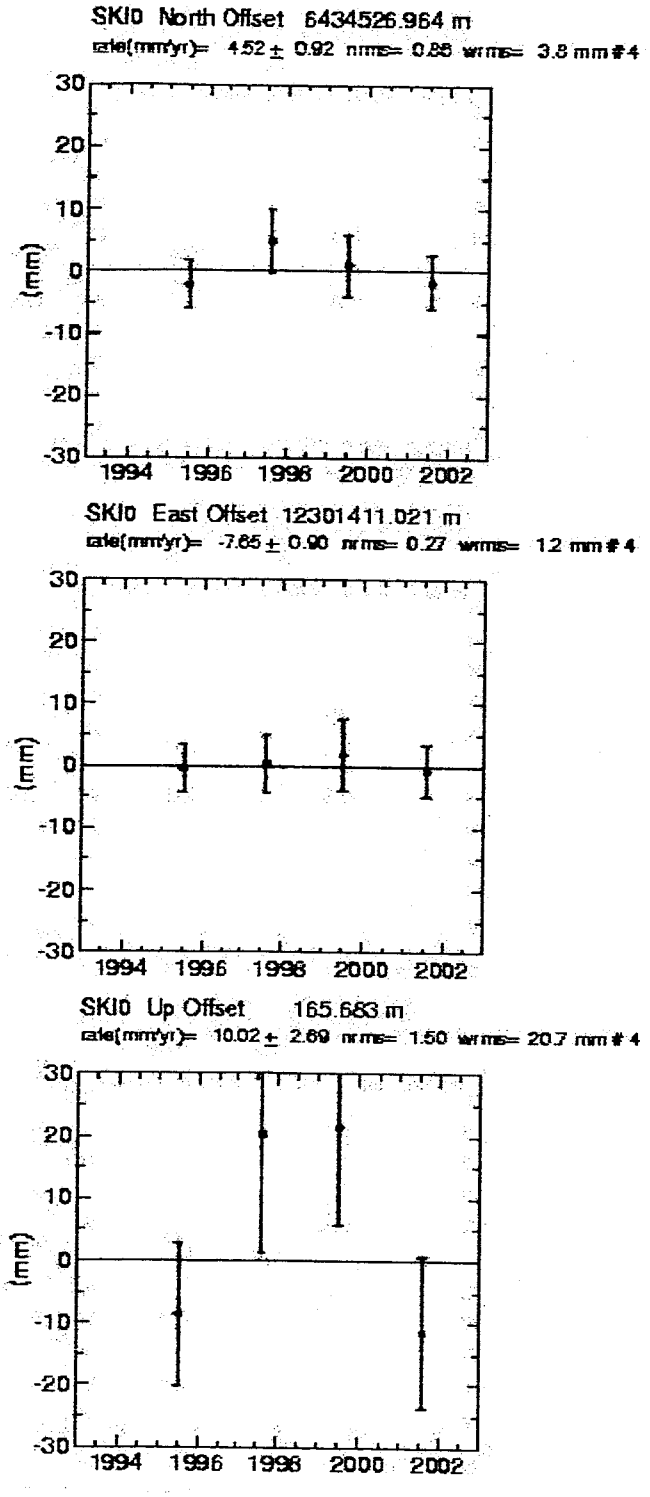
SKIO North Offset 6434526.964 m
rate(mm/yr)= 4.52 ± 0.92 nrms= 0.86 wrms= 3.8 mm # 4
30
20
10
0
-10
-20
-30
(mm)
1994
1996
1998
2000
2002
SKIO East Offset 12301411.021 m
rate(mm/yr)= -7.65 ± 0.90 nrms= 0.27 wrms= 1.2 mm # 4
30
20
10
0
-10
-20
-30
(mm)
1994
1996
1998
2000
2002
SKIO Up Offset 165.683 m
rate(mm/yr)= 10.02 ± 2.69 nrms= 1.50 wrms= 20.7 mm # 4
30
20
10
0
-10
-20
-30
(mm)
1994
1996
1998
2000
2002

Figure 3j

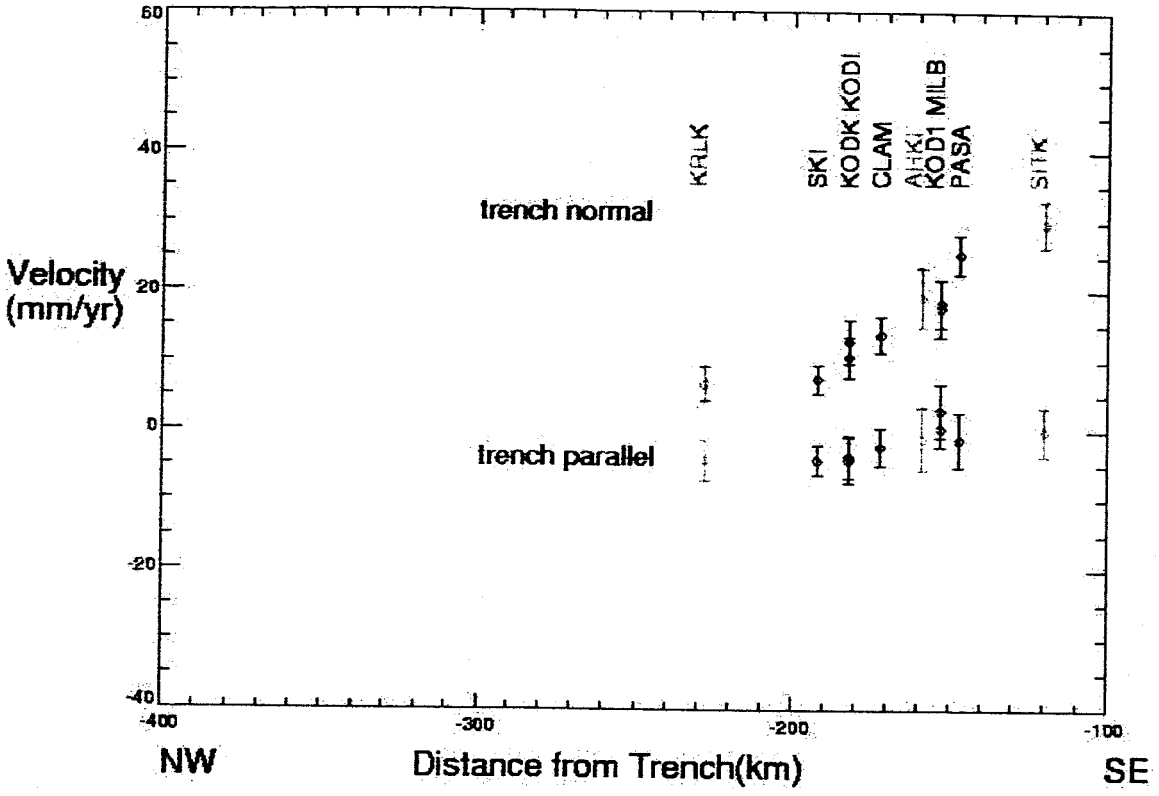
60
40
20
0
-20
-40
Velocity
(mm/yr)
KRLK
SKI
KODK
KODI
CLAM
AHKI
KOD1
MILB
PASA
SITK
trench normal
trench parallel
-400
-300
-200
-100
NW
Distance from Trench(km)
SE

Figure 4

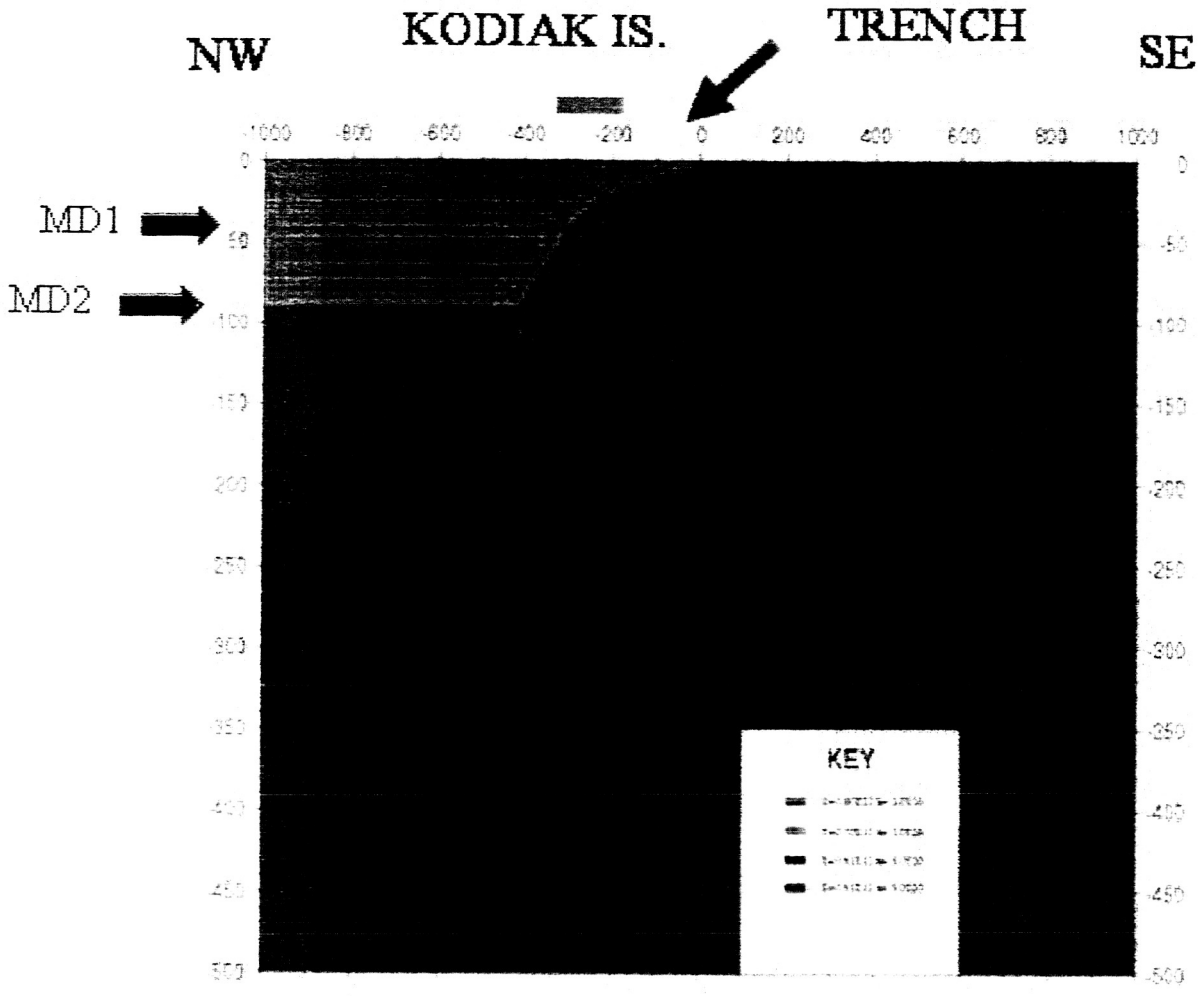

Figure 5a

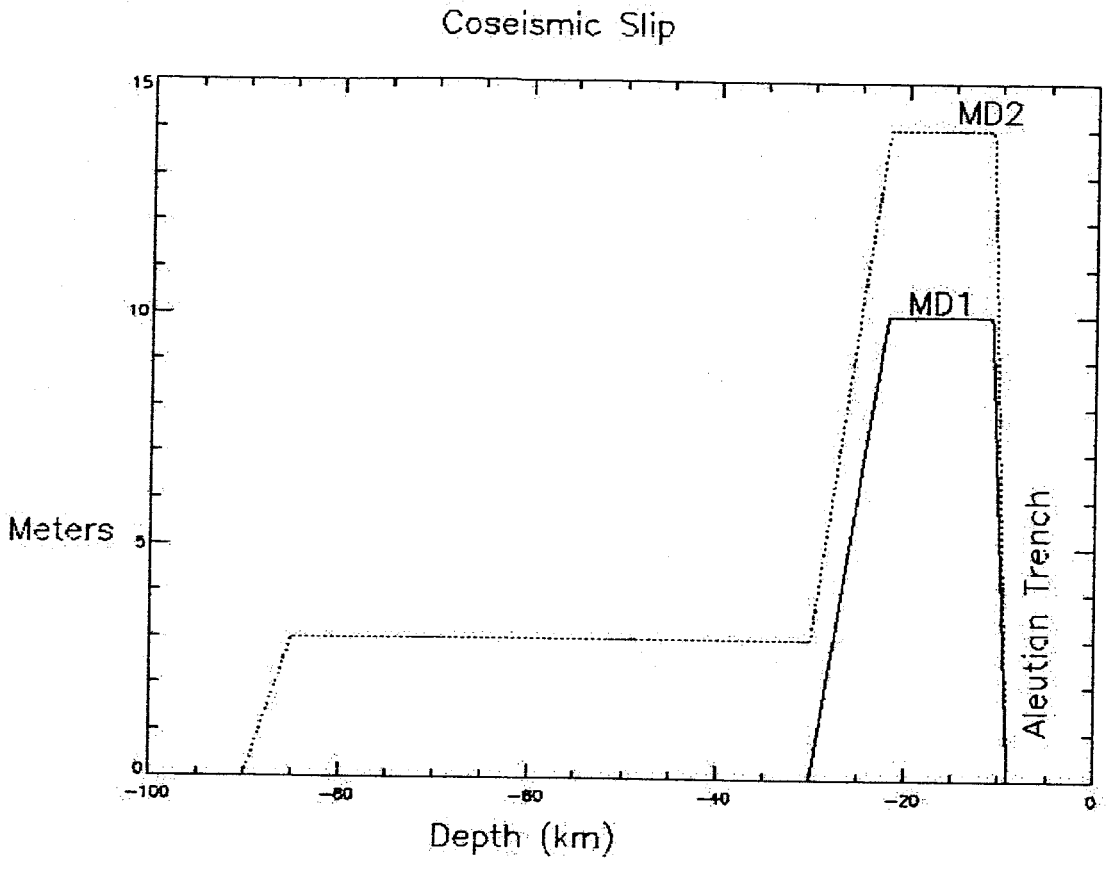
Coseismic Slip
MD2
MD1
Aleutian Trench
Meters
Depth (km)
15
10
5
0
-100
-80
-60
-40
-20
0

Figure 5b

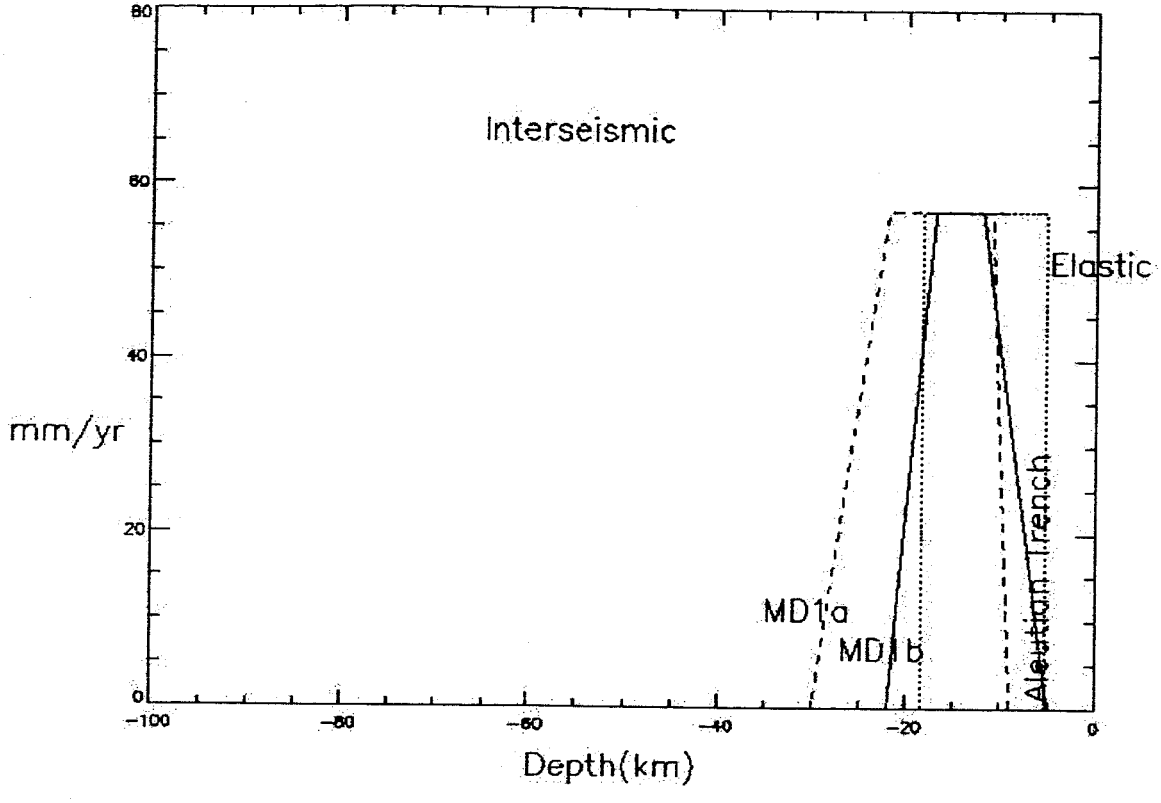
Interseismic
Elastic
MD1a
MD1b
Aleutian Trench
mm/yr
Depth(km)
80
60
40
20
0
-100
-80
-60
-40
-20
0

Figure 5c

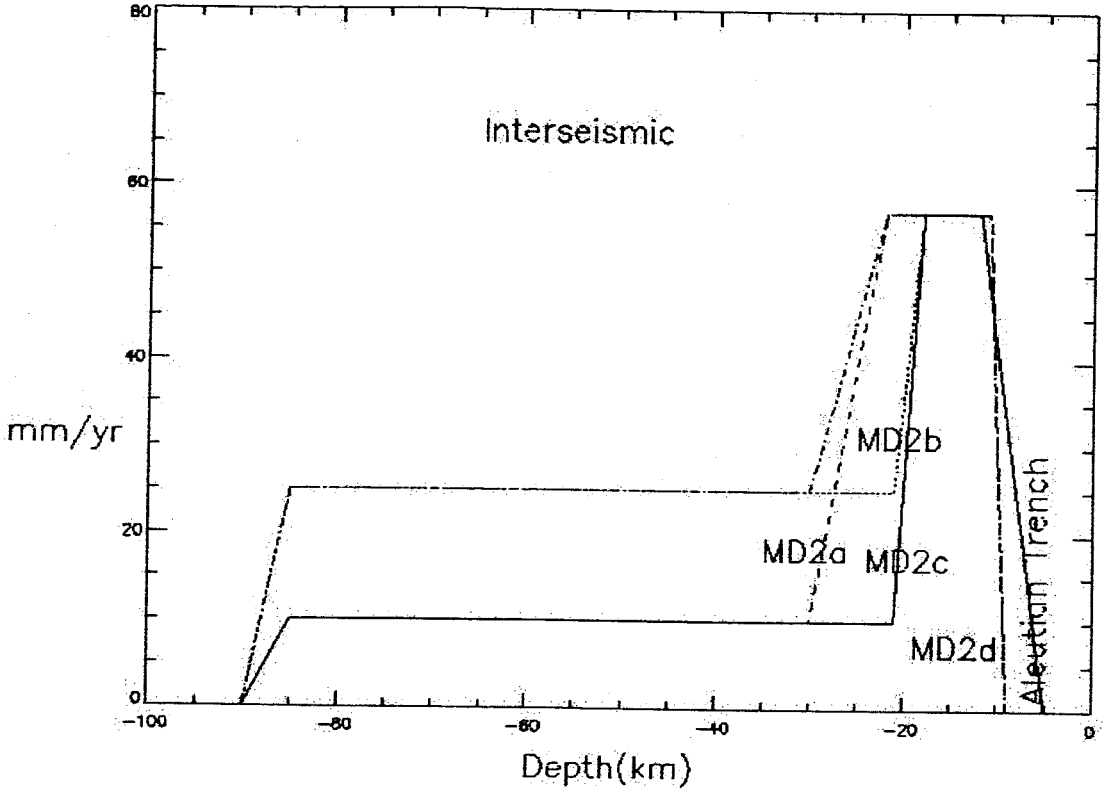
Interseismic
mm/yr
MD2b
MD2a
MD2c
MD2d
Aleutian Trench
Depth(km)
80
60
40
20
0
-100
-80
-60
-40
-20
0

Figure 5d

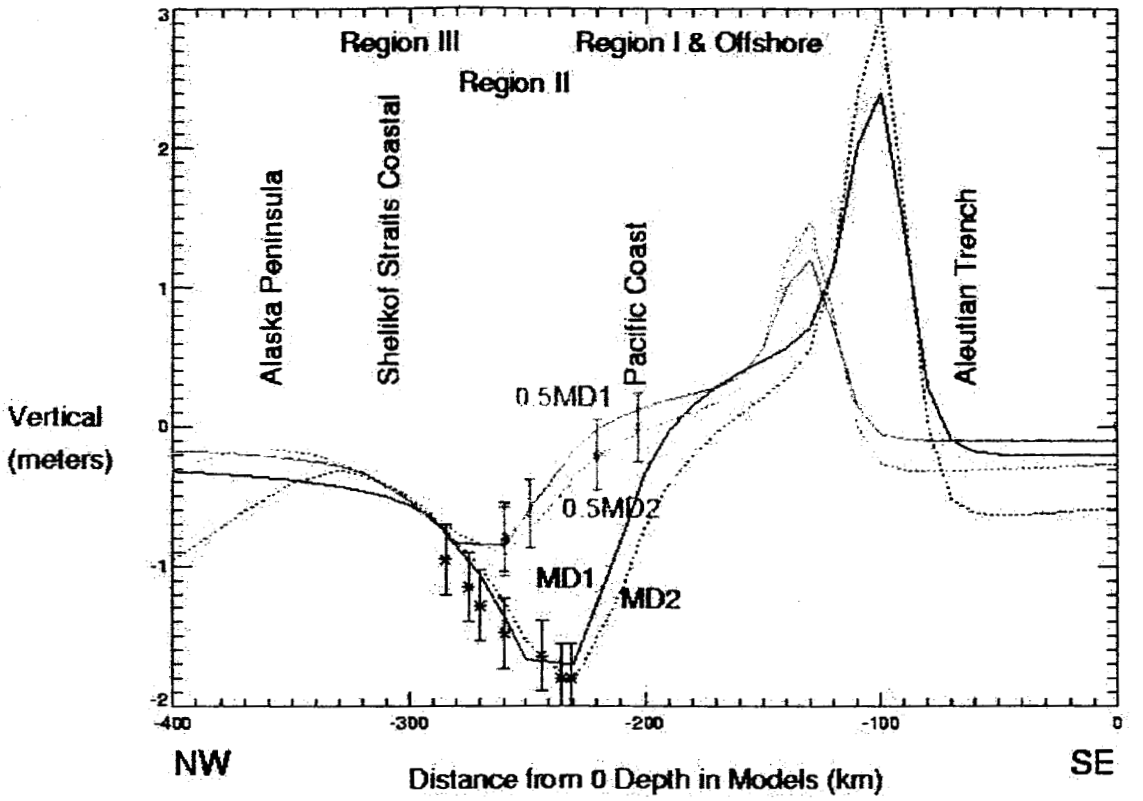
Region III
Region I & Offshore
Region II
Alaska Peninsula
Shelikof Straits Coastal
Pacific Coast
Aleutian Trench
0.5MD1
0.5MD2
MD1
MD2
Vertical
(meters)
3
2
1
0
-1
-2
-400
-300
-200
-100
0
NW
SE
Distance from 0 Depth in Models (km)

Figure 6

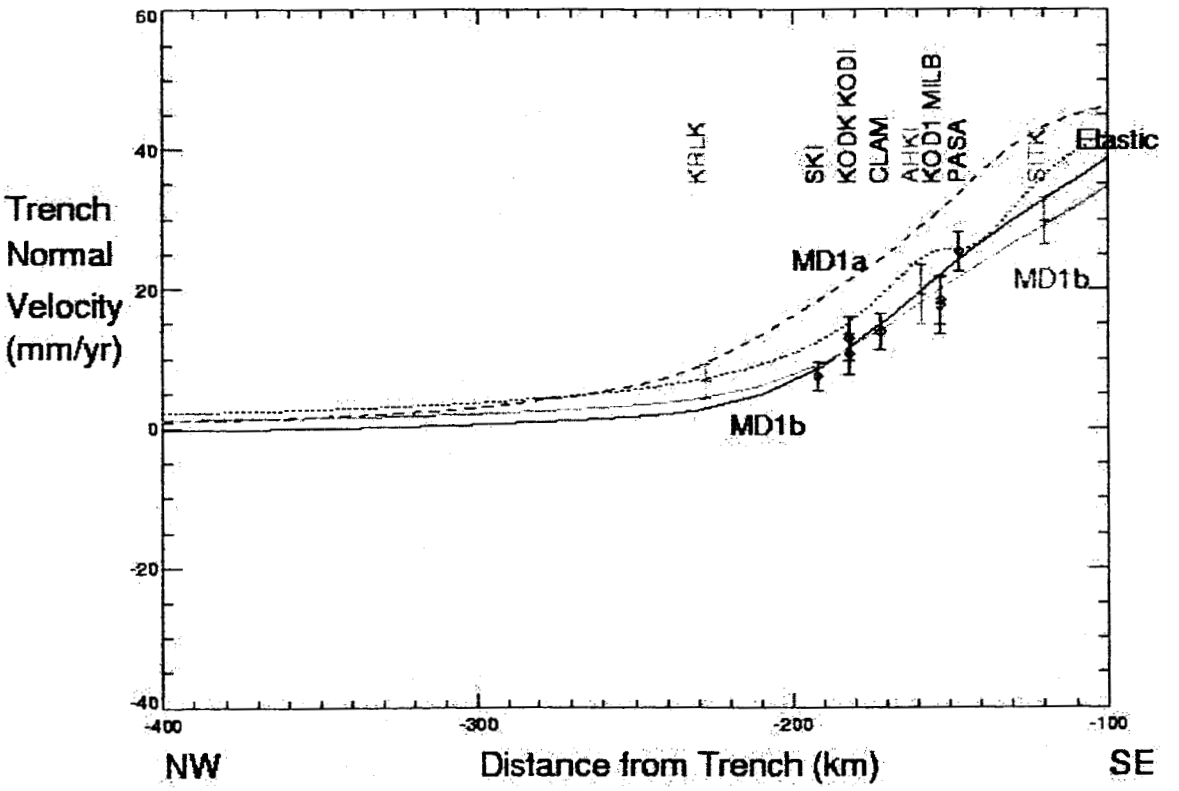
Trench
Normal
Velocity
(mm/yr)
60
40
20
0
-20
-40
-400
-300
-200
-100
NW
Distance from Trench (km)
SE
KRLK
SKI
KODK
KODI
CLAM
AHKI
KOD1
MILB
PASA
SITK
Elastic
MD1a
MD1b
MD1b

Figure 7a

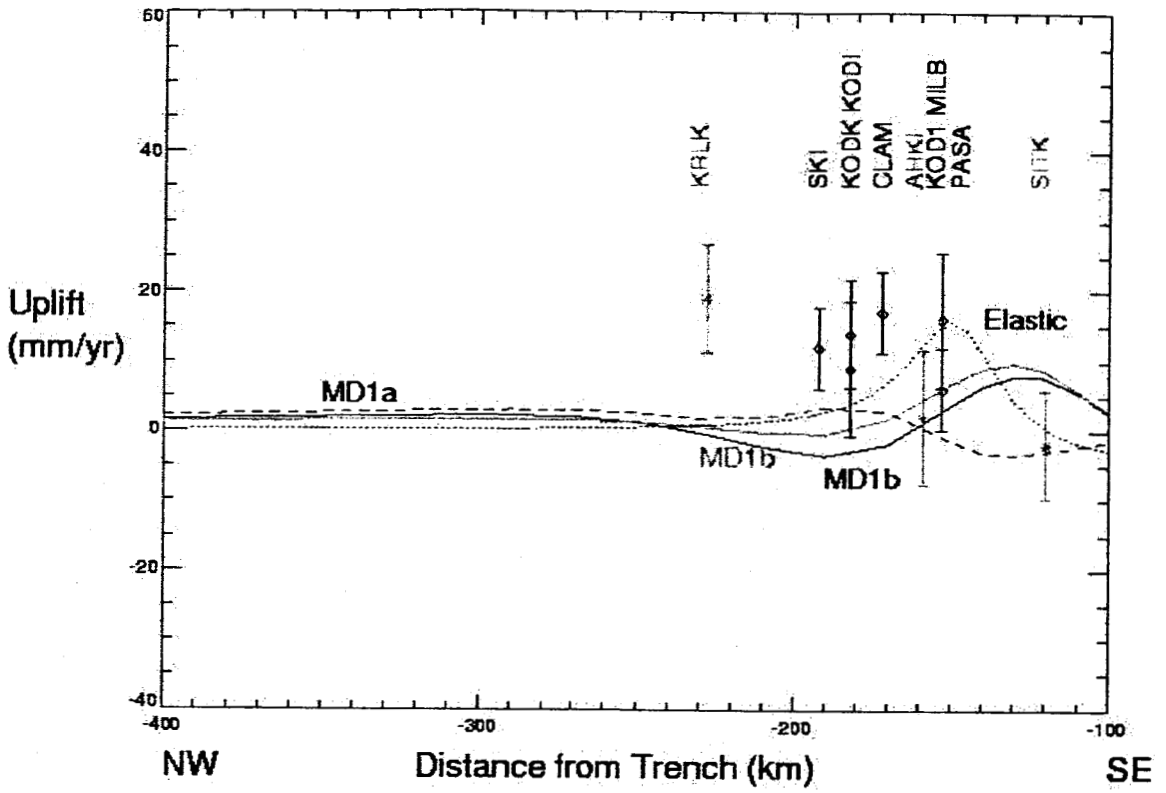
Uplift
(mm/yr)
60
40
20
0
-20
-40
-400
-300
-200
-100
NW
Distance from Trench (km)
SE
KALK
SKI
KODK
KODI
CLAM
AHKI
KOD1
MILB
PASA
SITK
Elastic
MD1a
MD1b
MD1b

Figure 7b

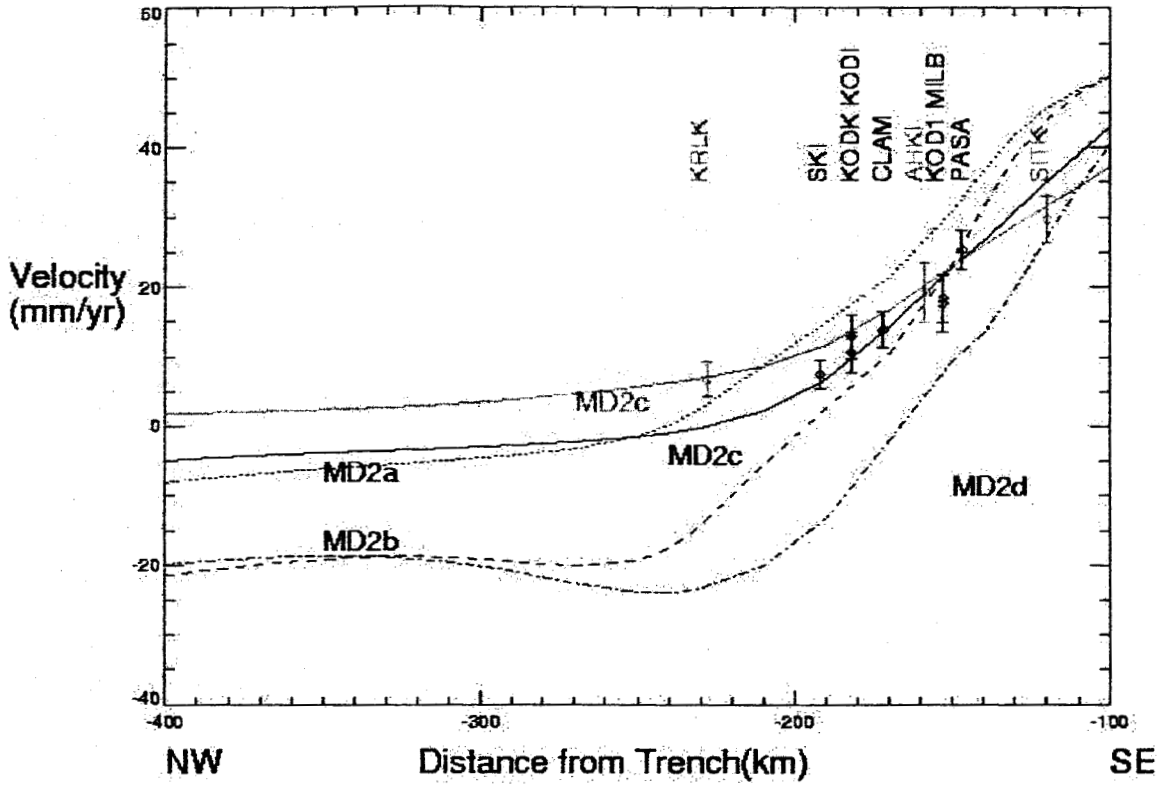
60
40
20
0
-20
-40
-400
-300
-200
-100
Velocity
(mm/yr)
NW
Distance from Trench(km)
SE
KRLK
SKI
KODK
KODI
CLAM
AHKI
KOD1
MILB
PASA
SITK
MD2c
MD2a
MD2b
MD2c
MD2d

Figure 8a

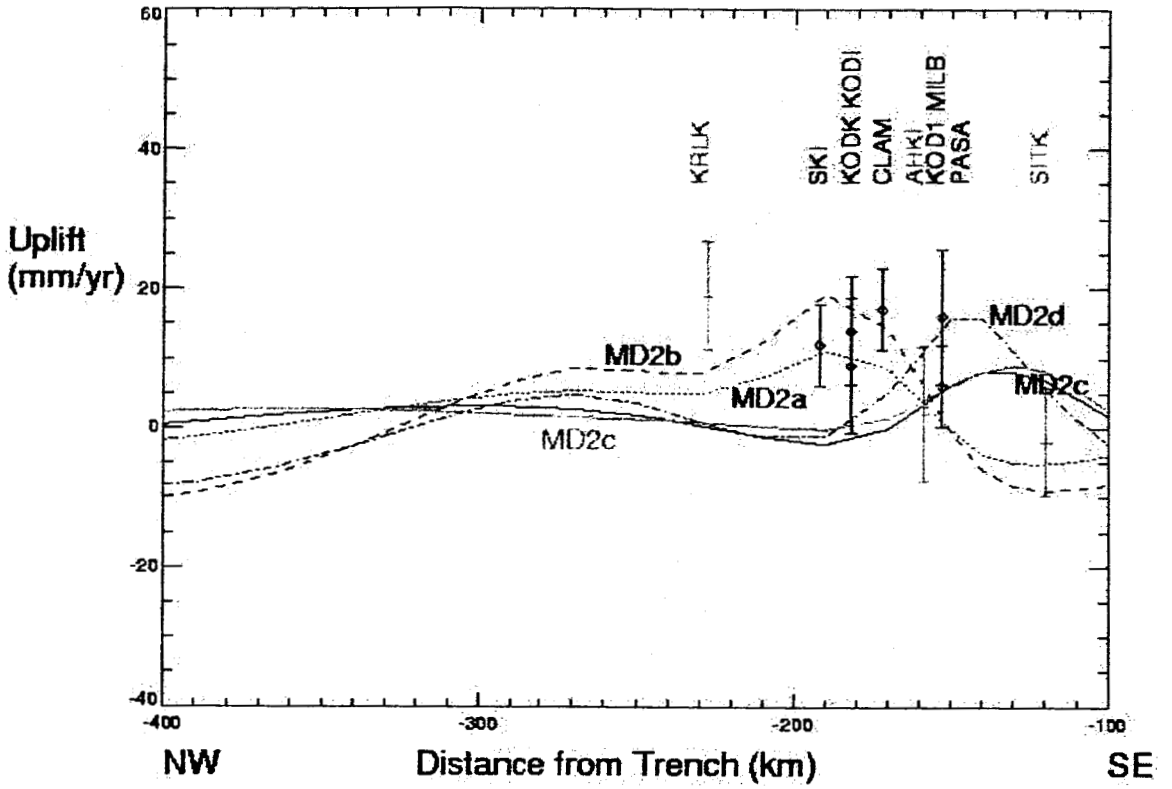
Uplift
(mm/yr)
60
40
20
0
-20
-40
-400
-300
-200
-100
NW
Distance from Trench (km)
SE
KRUK
SKI
KODK
KODI
CLAM
AHKI
KOD1
MILB
PASA
SITK
MD2b
MD2a
MD2c
MD2d
MD2c

Figure 8b

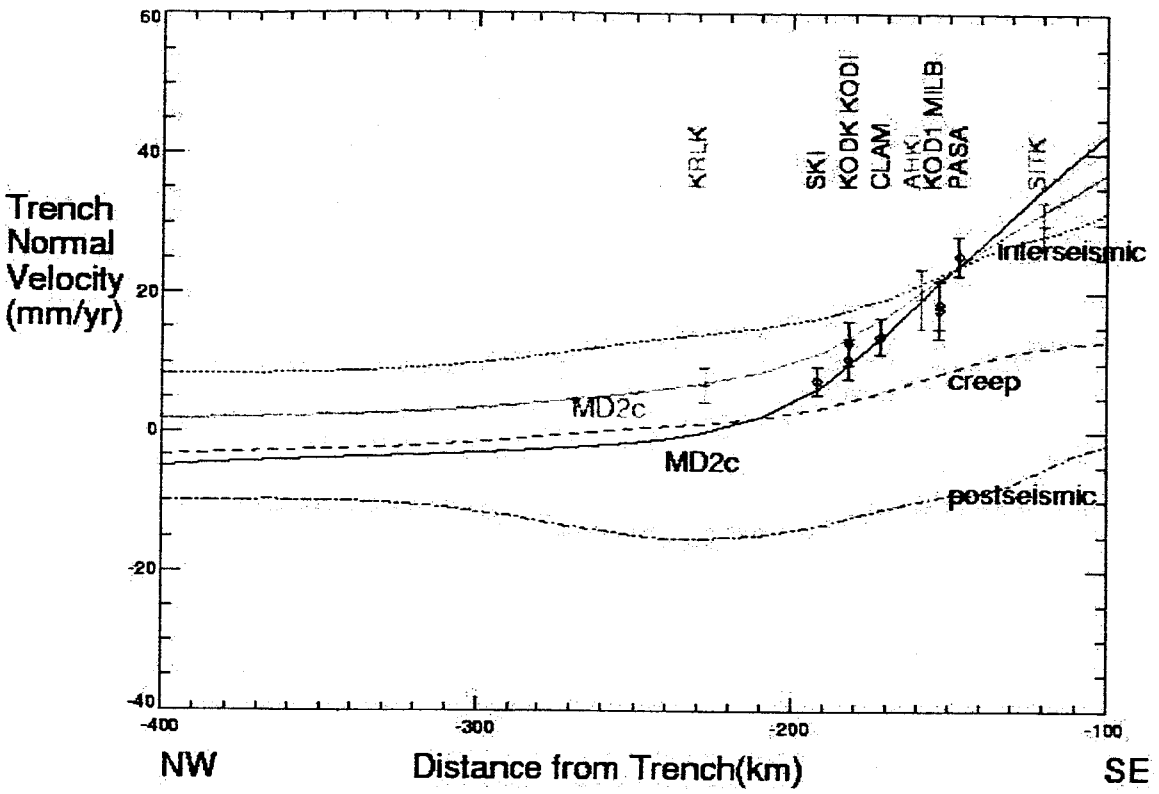
Trench
Normal
Velocity
(mm/yr)
60
40
20
0
-20
-40
-400
-300
-200
-100
NW
Distance from Trench(km)
SE
KRLK
SKI
KODK
KODI
CLAM
AHK
KOD1
MILB
PASA
SITK
interseismic
creep
MD2c
MD2c
postseismic

Figure 8c

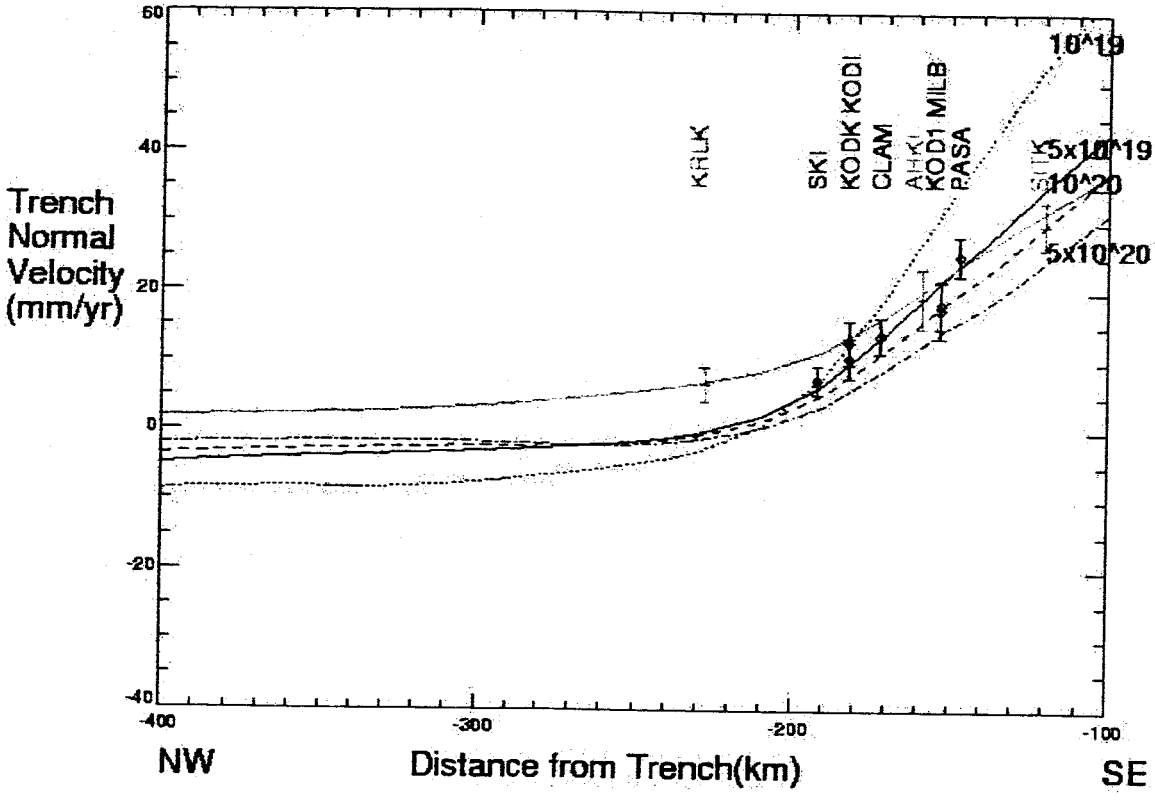
Trench
Normal
Velocity
(mm/yr)
60
40
20
0
-20
-40
-400
-300
-200
-100
NW
Distance from Trench(km)
SE
KRLK
SKI
KODK
KODI
CLAM
AHKI
KOD1
MILB
RASA
SITK
10^19
5x10^19
10^20
5x10^20

Figure 8d

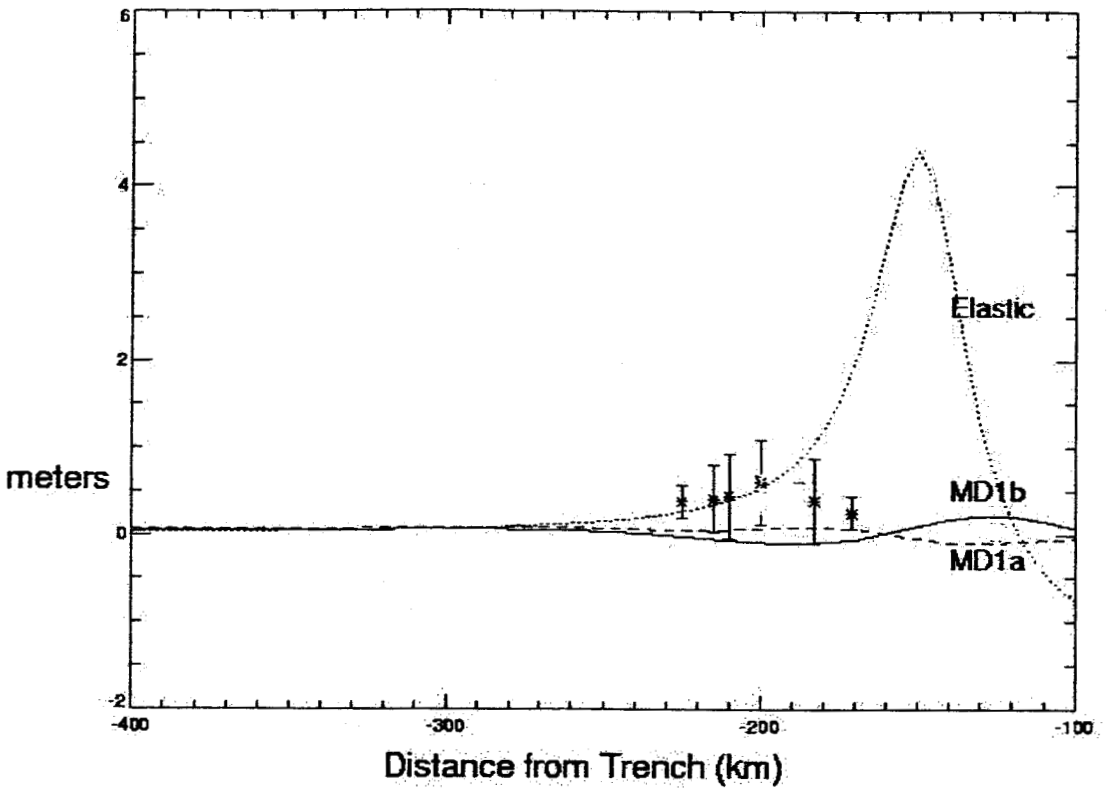
6
4
2
0
-2
meters
-400
-300
-200
-100
Distance from Trench (km)
Elastic
MD1b
MD1a

Figure 9a

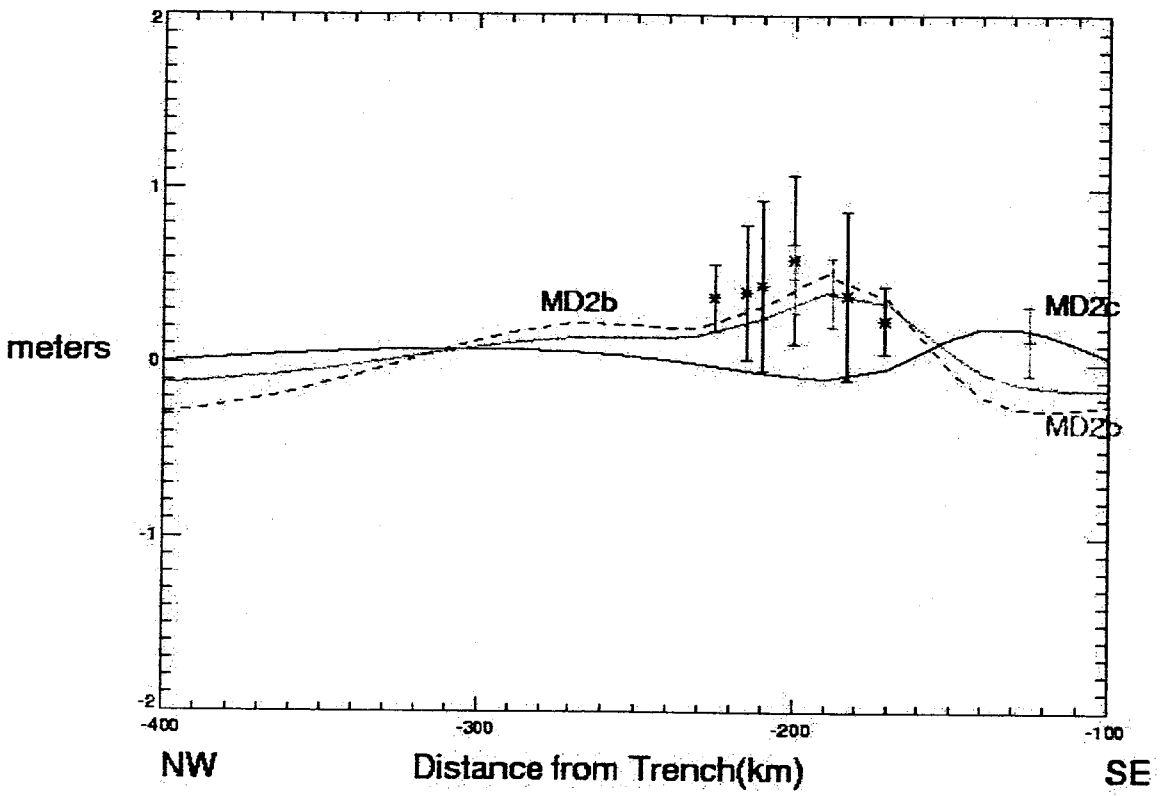
meters
2
1
0
-1
-2
MD2b
MD2c
-400
-300
-200
-100
NW
Distance from Trench(km)
SE

Figure 9b

Popular Summary of "Crustal Deformation and the Seismic Cycle across the Kodiak Islands, Alaska" by J. Sauber(NASA GSFC), G. Carver (Humboldt University), S. Cohen (NASA GSFC) and R. King (MIT)

The Kodiak Islands are located approximately 120 to 250 km from the Alaska-Aleutian Trench where the Pacific plate is underthrusting the North American plate at a rate of about 57 mm/yr. The southern extent of the 1964 Prince William Sound ($M_w = 9.2$) earthquake rupture occurred offshore and beneath the eastern portion of the Kodiak Islands. In this study we report global positioning system (GPS) results (1993-2001) from northern Kodiak Island that span the transition between the 1964 uplift region along the eastern coast and the region of coseismic subsidence further inland. We used these geodetic results to look at the amount of slip near Kodiak during the great 1964 earthquake and we examined the relation of the coseismic slip to crustal deformation measured in the 30 years following the great earthquake. In addition to strain accumulating that will be released in the next large subduction earthquake, we suggest that 4-8 mm/yr of slip is accumulating that will be released as left-lateral strike-slip motion across the inland faults of Kodiak Island. Based on the pre-1964 and post-1964 earthquake history, as well as the pattern of interseismic earthquakes across the plate boundary zone, we hypothesize that in southern Kodiak some strain is released in moderate to large earthquakes between the occurrences of great earthquakes like the 1964 event. In northern Kodiak, however, the main thrust zone is locked and will eventually be relieved in another large subduction zone earthquake in the future.